6.05 Heat Flow and Thermal Structure of the Lithosphere

C. Jaupart, Institut de Physique du Globe de Paris, Paris, France

J.-C. Mareschal, GEOTOP-UQAM-McGill, Montreal, QC, Canada

6.05.1 Introduction

Over the past 200 years, the cooling of the Earth has been the object of many studies (Fourier, 1820; Thomson, 1864; Strutt, 1906; Holmes, 1915; McDonald, 1959; Urey, 1964; Birch, 1965). Since the paper of Kelvin (Thomson, 1864), the estimate of the average heat flux has changed by a factor of less than 2, but our understanding of this value and its implication for the Earth's thermal structure has been turned upside down several times. Kelvin obtained the solution of the heat equation for the conductive cooling of a half-space, initially at constant temperature, after a sudden drop in surface temperature. Because heat flux varies as $1/\sqrt{\text{time}}$, Kelvin used the present heat flux to determine the age of the Earth. The Kelvin model is not correct for two reasons. One is that the Earth is not cooling by conduction only; convective motions are driven by temperature differences in the mantle. Another reason is that Kelvin ignored internal heat sources; the amount of heat generated by the radioactive decay of U, Th, and K in silicate rocks accounts for a large fraction of the heat flow. This was first pointed out by Strutt (1906) who estimated from heat-production measurements that crustal thickness could not exceed 60 km. Following Bullard (1939, 1954) and Revelle and Maxwell (1952), systematic heat flow measurements on land and at sea were undertaken which showed that radiogenic heat production is not uniformly distributed. It is worth noting that in the 1950s, when Bullard undertook oceanic heat flux measurements, he expected heat flux to be lower in the oceans than in the continents, because the oceanic crust is thin and poor in radioelements.

The concept of lithosphere, as seen from the thermal standpoint, and estimates for its thickness have also evolved. The heat flux data do not fit the age variation predicted by the half-space conductive cooling model. In the oceans, this is because heat is brought to the base of the lithosphere, probably through small-scale convection. In the continents, variations of heat flux with age are obscured by large changes of radiogenic heat production in the crust.

How continents and oceans deform and are affected by magmatism depends largely on their thermal structures. Thus, current research on geological and geodynamical processes requires accurate knowledge of temperatures in specific regions. Despite many decades of measurements, many geological provinces on the continents and large parts of the oceans remain poorly sampled. Two methods have been used to circumvent this data gap. One has been to search for a simple control variable on lithospheric temperatures, such as age. Another has been to develop increasingly precise and detailed seismic velocity profiles and to invert them for temperature.

To set the stage for this chapter, we recapitulate briefly the advances made in one generation, as measured against a comprehensive review paper (Sclater *et al.*, 1980). When that review was published, the oceanic heat flow problem was essentially solved. Since then, the model has passed a series of critical tests. For young sea floor, this has entailed documenting and understanding hydrothermal circulation through fractured oceanic crust buried by variable thickness of low-permeability sediments and determination of small-scale heat flux variations. For old sea floor, this has involved precise measurements of heat flux through areas with flat topography unaffected by sedimentary perturbations (slumping, turbidity currents) and deep oceanic currents. On continents, progress has been made thanks to systematic measurements of heat flux and heat production in old cratons and determination of (P, T) conditions in the lithospheric mantle through xenolith studies. Additionally, subsidence studies in a large number of sedimentary basins have documented the transient response of the continental lithosphere to thermal perturbations. For both continents and oceans, detailed seismic velocity profiles have been interpreted in terms of the thermal structure of the lithosphere and mantle. Complementary information has come from many disciplines, leading to a very large data set and to a sound understanding of key issues.

Here, we review these advances focusing on two issues. One is to assess the reliability of age as a control variable on heat flow and lithospheric thermal structure. In continents, variations of crustal heat production are large in both the horizontal and vertical directions and prevent the calculation of a single typical 'geotherm' for all provinces of the same age. In oceans, age is the main control variable but small variations remain due to lateral variations of mantle temperature. The other issue is the control on lithospheric thickness and the mechanism of heat transport at the base of the lithosphere – in other words, the bottom boundary condition to be used in thermal models. In steady state, this boundary condition is of small concern because the thermal structure can be determined by downward

continuation of surface measurements. It is a major factor, however, if the thermal regime is transient.

We have not aimed this chapter at heat flow specialists and pursue two different goals. One is to show how to use heat flux data, which involves an analysis of available measurements and their uncertainties as well as a discussion of missing information. Our other goal is to illustrate the controls on the different thermal regimes that are observed and to describe the key steps in data interpretation. This will be achieved with simple physical arguments instead of complicated numerical calculations. In the following, for simplicity, data and measurements refer only to heat flow studies unless otherwise specified.

6.05.2 Surface Heat Flux and Heat Transport in the Earth

6.05.2.1 Distribution of Heat Flux: Large-Scale Overview

There are more than 20 000 heat flux measurements at Earth's surface, distributed about equally between continents and oceans (Pollack *et al.*, 1993). The heat flow map of North America (**Figure 1**) (Blackwell and Richards, 2004) illustrates the differences between continental and oceanic heat flow. Except in active regions (Basin and Range, Yellowstone, Rio Grande Rift, etc.), heat flux is low throughout the North American continent and lowest in the Canadian Shield. In contrast, heat flux is higher in the oceans than in the continents, and higher on the western than on the eastern margin. In addition to these large-scale differences, many other features need detailed interpretation. We shall see that one cannot apply the same physical frame-work and the same interpretation methods to oceans and continents. From a global perspective, the oceanic lithosphere is in a transient thermal state over most of its short residence time at the Earth's surface, contrary to continents which are mostly in, or close to, thermal steady state. Oceanic heat flux follows a decreasing trend as a function of age which parallels that of elevation (or bathymetry). The continental lithosphere has experienced a longer evolution and is characterized by a complicated structure and composition. More importantly, the continental crust is enriched in radioactive elements which contribute

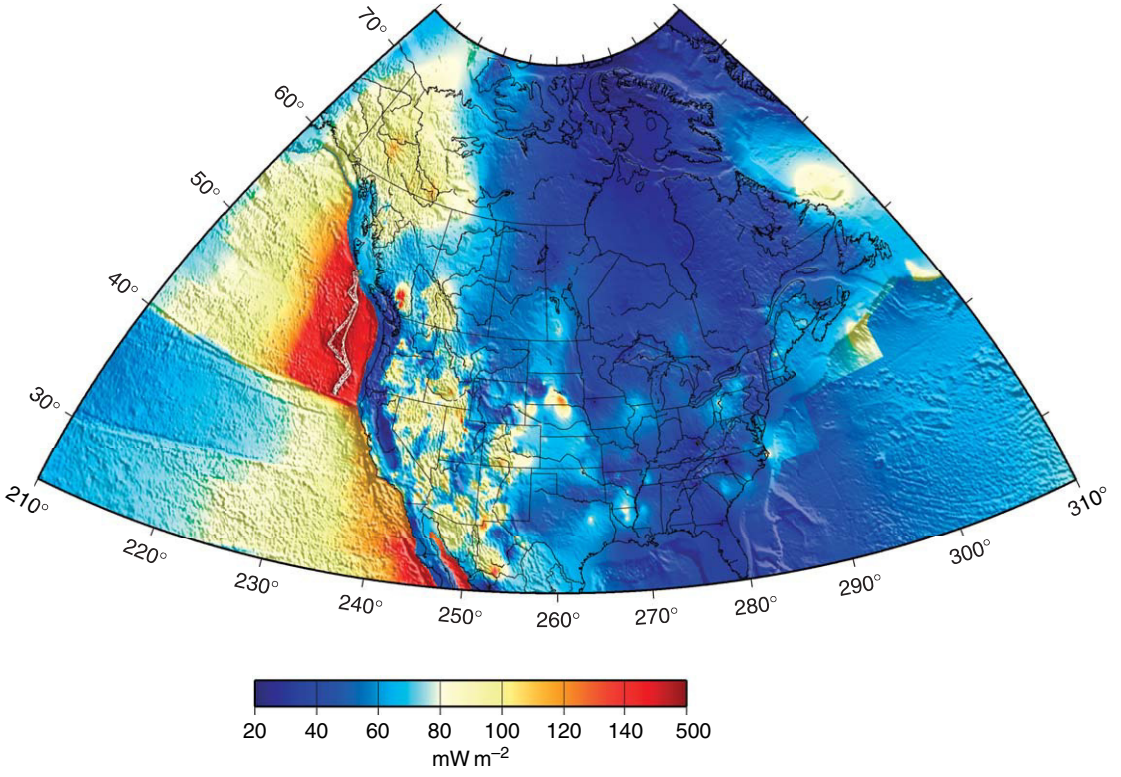

Figure 1 Heat flow map of North America. Adapted from Blackwell D and Richards M (2004) Geothermal map of North America, NewYork: Plenum.

the largest component to the surface heat flow. Continental elevation is controlled mainly by variations of crustal thickness and composition, and depends weakly on thermal structure.

The raw averages of oceanic and continental heat flux data are 70 and 80 mW m^{-2}, respectively (Sclater *et al.*, 1980; Pollack *et al.*, 1993; Harris and Chapman, 2004). These numbers are biased for several reasons. Only the conductive component of the heat flow can be measured. In the oceans, heat flux measurements are made in sediments where conductive conditions prevail, but hydrothermal circulation and associated advective heat transport may be very active in the igneous crust beneath. For this reason, raw heat flux data are not reliable in lithospheric studies and one must depend on small-scale experiments to account for the effects of hydrothermal convection. Once this is done, the average oceanic heat flux is found to be 101 mW m^{-2}. In the continents, high heat flow regions that cover a small surface are oversampled. Excluding the values from the US, where many values were obtained in the Basin and Range Province, the mean continental heat flux drops to only 65 mW m^{-2}. The sampling bias can also be removed by weighting the data by area, as demonstrated in **Table 1**. Averaging over $1^\circ \times 1^\circ$ windows yields a mean continental heat flux of 65.3 mW m^{-2}. This mean value does not decrease significantly when averaging is done over wider windows. The histograms of heat flux values or averages over $1^\circ \times 1^\circ$ windows have identical shapes, except for the extremely high values (>200 mW m^{-2}).

Table 1 Continental heat flux statistics[a]

	μ(**Q**) (mW m^{-2})	σ(**Q**) (mW m^{-2})	N(**Q**)
World			
All values	79.7	162	14 123
Averages $1^\circ \times 1^\circ$	65.3	82.4	3024
Averages $2^\circ \times 2^\circ$	64.0	57.5	1562
Averages $3^\circ \times 3^\circ$	63.3	35.2	979
USA			
All values	112.4	288	4243
Averages $1^\circ \times 1^\circ$	84	183	532
Averages $2^\circ \times 2^\circ$	78.3	131.0	221
Averages $3^\circ \times 3^\circ$	73.5	51.7	128
Without USA			
All values	65.7	40.4	9880
Averages $1^\circ \times 1^\circ$	61.1	30.6	2516
Averages $2^\circ \times 2^\circ$	61.6	31.6	1359
Averages $3^\circ \times 3^\circ$	61.3	31.3	889

[a]μ is the mean, σ is the standard deviation, and N is the number of values.

6.05.2.2 Mechanisms of Heat Transport

In the solid Earth, three mechanisms of heat transport must be accounted for. Ordered by increasing depth, these are hydrothermal convection, conduction, and convection. Hydrothermal circulation develops in fractures and pores, which get closed by the confining pressure deeper than 10 km. This mechanism is of little importance at the lithospheric scale but plays a crucial role in shallow environments where heat flux measurements are made. Conduction dominates over regions that are cold and cannot be deformed over geological timescales. One can see here the strong link between thermal and mechanical processes. At sufficient depth, the temperature is high enough for rocks to deform at significant rates and convective heat transfer dominates. In active volcanic areas, one must account for yet another heat transport mechanism: magma ascent.

6.05.2.3 Thermal Boundary Layer Structure

As will be shown later, heat is brought to the base of the lithosphere by convection in the mantle beneath both continents and oceans. The vertical temperature profile must be divided into two parts: an upper part where heat is transported by conduction and a lower convective boundary layer. In steady state and in the absence of heat-producing elements, heat flow is constant in the conductive upper part, implying a constant temperature gradient for constant thermal conductivity. In contrast, the temperature gradient is not constant in the convective boundary layer and progressively tends to a small value in the mantle beneath. For definition of the thermal lithosphere, we must consider three different depths (**Figure 2**). The shallowest boundary, b_1, corresponds to the lower boundary of the conductive upper part and of what we shall call the thermal lithosphere. The deepest boundary, b_3, corresponds to the lower limit of the thermal boundary layer. This boundary may also be regarded as the transition between the lithospheric regime and the fully convective mantle regime, such that the mantle thermal structure below is not related to that of the lithosphere. An intermediate depth, b_2, is obtained by downward extrapolation of the conductive geotherm to the isentropic temperature profile for the convecting mantle. With no knowledge of boundary layer characteristics, one can only

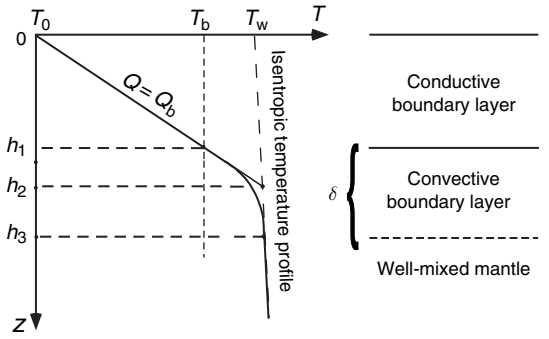

Figure 2 Schematic structure of the thermal boundary layer at the top of Earth convecting mantle. The boundary layer must be split into two parts. In the effectively rigid upper part of thickness h_1, heat is transported by conduction. In the unstable lower part of thickness $\delta = h_3 - h_1$, heat is brought to the base of the upper part through convection. The vertical profile obtained by downward extrapolation of shallow temperature data intersects the well-mixed isentropic profile at yet another depth, h_2. The temperature at the base of the conductive upper part is T_b, which is significantly smaller than the well-mixed potential temperature T_w. The temperature difference across the unstable boundary layer of thickness δ is $T_w - T_b$.

determine h_2 and h_3, the former from heat flow data and the latter from seismic velocity anomalies. Such determinations are associated with two major caveats. One is that they cannot be equal to one another, which does not permit cross-checks. The other caveat is that they say nothing about h_1. Yet, it is h_1 which defines the mechanically coherent unit (the 'plate') which moves at Earth's surface and sets the thermal relaxation time which follows tectonic and magmatic perturbations. Uncertainty on this thickness has severe consequences because the diffusive relaxation time is $\propto h^2$. A final remark is that h_1 characterizes the upper boundary condition at the top of the convecting mantle.

6.05.2.4 Basal Boundary Conditions

In steady state, the heat flux at Earth's surface is equal to

$$Q_0 = Q_{\text{crust}} + Q_{\text{lith}} + Q_b \qquad [1]$$

where Q_{crust} and Q_{lith} stand for the contributions of heat sources in the crust and in the lithospheric mantle, and Q_b is the heat flux at the base of the lithosphere. In the oceans, one may ignore the first two with negligible error and surface heat flux is a direct measure of the basal heat flux. In the continents, the procedure is more complex because it involves estimating the potentially large crustal contribution, Q_{crust}. In both cases, steady state cannot be taken for granted because it depends on the lithosphere thickness, which is part of the solution. Thus, in practice, one must first demonstrate that transient thermal effects are negligible.

Far from steady-state conditions, the surface heat flux includes a large transient component and identifying the different components is an underconstrained problem. In other words, a purely empirical approach is not sufficient and measurements can only be interpreted within a theoretical framework. This major difficulty has been at the core of heat flux studies for the last three decades. From a physical point of view, one must introduce three temperatures, T_0 at the upper boundary, which, for all practical purposes, may be taken as fixed and equal to 0°C, T_b at the base of the lithosphere, and T_w in the well-mixed convective interior. In steady state and in the absence of heat sources, one has

$$Q_0 = Q_b = k\frac{T_b - T_0}{h_1} \qquad [2]$$

where k is the thermal conductivity. A closure equation relates this flux to the temperature difference across the convective boundary layer, $(T_w - T_b)$ (**Figure 2**). In the general case, this involves solving for the fully coupled heat transfer problem, which requires comprehensive convection models involving a variety of scales. Numerical models of this kind remain tentative because of the uncertainties in the setup (initial conditions, rheological properties, accounting for continents and oceans, etc.) as well as inherent computer limitations. For this reason, simple models have been developed and applied locally to a subset of observations. A common procedure is to introduce a heat transfer coefficient B:

$$Q_b = B(T_w - T_b) \qquad [3]$$

Two limiting cases have been considered. For perfectly efficient heat transfer, $B \to \infty$, implying that $T_b \to T_w$. This is the fixed-temperature boundary condition. Another limit case is when the convective mantle can only maintain a fixed heat flux. In this case, Q_b is set to a constant. Both boundary conditions allow straightforward solutions to the heat equation if the lithosphere thickness is fixed. One additional problem is to ascertain whether or not the lithosphere thickness changes with time, which requires an understanding of the physical controls on lithosphere thickness.

6.05.2.5 Controls on Lithosphere Thickness

We know of three controlling factors, which have been studied to varying degrees of complexity. One is the strong temperature dependence of rheological properties, such that only the least viscous (and hence hottest) part of the thermal boundary layer breaks down and sustains small-scale convection at the base of a stable upper layer (Parsons and McKenzie, 1978). With a reliable rheological law, one can calculate all characteristics of the thermal boundary layer, including thickness h_1 and basal heat flux Q_b. Uncertainties in upper-mantle properties have led to reversing the approach, in such a way that heat flux data have in fact been used to obtain constraints on mantle rheology (Davaille and Jaupart, 1994; Solomatov and Moresi, 2000; Huang and Zhong, 2005). A second mechanism relies on an intrinsic density difference such that the plate is made of buoyant material which cannot become unstable upon cooling (Jordan, 1975; Oxburgh and Parmentier, 1977; Jordan, 1981). In a third mechanism, a 'compositional' rheological contrast stabilizes the plate such that it is more viscous than the mantle below (Pollack, 1986; Hirth and Kohlstedt, 1996). All three mechanisms are relevant in the Earth but so far have rarely been included together in convection calculations. The interesting question is to assess the importance of each one of them. Current limitations on the resolving power of geophysical studies and on how the physical properties of lithospheric material vary as a function of temperature, composition, and water content prevent firm conclusions. Useful information can be gained by invoking the physical processes of continental root formation.

Mantle material upwelling beneath an oceanic ridge undergoes partial melting and basalt extraction, leaving a residue that is both slightly buoyant (Oxburgh and Parmentier, 1977; Schutt and Lesher, 2006) and more viscous than the underlying mantle (Hirth and Kohlstedt, 1996). Depending on mantle temperature and water content, melting may start at depths between about 60 and 80 km which sets the thickness of the buoyant and viscous residue. Naturally, one must ask whether this is equal to h_1, the thickness of the thermal lithosphere. As usual, the continental problem is more complicated because there is no consensus on the mechanism of formation of cratonic roots. One popular model is inspired by the oceanic one and invokes melting and melt extraction at the top of large mantle plumes. This case is analogous to that of oceanic ridges. According to an alternative model, continental lithosphere is generated by melting above subduction zones (Carlson *et al.*, 2005). The key consequence is that the proto-root may remain hydrated, in which case it is intrinsically buoyant but not intrinsically more viscous. Geoid anomalies over cratons provide evidence for a negative intrinsic density contrast (Turcotte and McAdoo, 1979; Doin *et al.*, 1996).

6.05.2.6 The Thermal Lithosphere as Opposed to the Seismically Defined Lithosphere

As will be illustrated in this chapter, knowledge of Earth's shallow thermal structure remains subject to large uncertainties, which has motivated the use of alternative methods. Among them, seismic methods are the most powerful and precise, but do not discriminate well between the different thicknesses involved (**Figure 2**).

On a worldwide scale, with very few exceptions, cratons are systematically associated with fast regions extending to depths of about 200–300 km. With reference to the schematic lithospheric structure given in **Figure 2**, such estimates correspond to depths $\geq h_3$, and hence provide upper bounds to both h_1 and h_2. The lithosphere preserves compositional heterogeneities in contrast to the well-mixed asthenosphere. Thus, its thickness can be defined by seismology as the depth where small-scale lateral heterogeneities disappear. Such depth would be $\geq h_1$. Discontinuities in the depth range 80–240 km have been observed by seismic reflection, refraction experiments, and by teleseismic body-wave studies. They cannot be explained by thermal effects but could be due to higher hydration in the asthenosphere, in which case they would correspond to h_1.

Independent information may come from the vertical distribution of seismic anisotropy. One may expect different anisotropy characteristics and orientation depending on depth (Gung *et al.*, 2003). Below the base of the lithosphere, anisotropy is due to convective shear stresses and should be aligned with the direction of plate motion. Within the lithosphere, anisotropy probably reflects a fabric inherited from past tectonic events (Silver, 1996). The depth at which the anisotropy characteristics change may therefore be interpreted as the base of the lithosphere, that is, $\geq h_1$.

Electrical conductivity profiles provide yet another means of constraining lithosphere thickness.

Conductivity is sensitive to both temperature and the water content of mantle rocks. Analysis of data from the Archean Slave Province, Canada, and the northeastern Pacific shows that old continental lithosphere contains less water than the oceanic mantle in the depth range 150–250 km (Hirth *et al.*, 2000).

6.05.2.7 Summary: Different Approaches to Thermal Studies of the Lithosphere

The thermal boundary layer at the Earth's surface must be divided into two parts with different rheologies and heat transport mechanisms. These differences are significant for three reasons. One is that different geophysical methods provide constraints on different parts of the boundary layer and hence cannot be compared without care. Another reason is that heat flow is not sensitive to the same parts of the boundary layer in transient and steady-state conditions. A third reason is that these two parts play different roles for the dynamics of mantle convection and for the secular cooling of the Earth. For example, mantle plumes must first go through the convective boundary layer before reaching the base of the lithosphere. Thus, for studies of plume penetration through the lithosphere, the relevant thermal perturbation is the sum of the temperature anomaly driving plume ascent through the deep mantle and the temperature difference across the boundary layer, which may be large.

For these reasons, a purely empirical approach to heat flux data is doomed to fail. The problem is more acute in continents because of crustal heat production, an independent variable unrelated to heat transport mechanisms. At the very least, heat flux data provide quantitative constraints on models derived from other observables. At best, when used in conjunction with other methods and some consideration of heat transport mechanisms, they provide insight on mantle dynamics.

6.05.3 Oceanic Heat Flux, Topography and Cooling Models

6.05.3.1 Data

Figure 3 shows the oceanic heat flux averages from Stein and Stein (1992), plotted as a function of age. Large data sets are already available, suggesting that more measurements would not reduce the scatter in the data. Measurement campaigns should now be targeted at addressing specific problems at the local scale. The main conclusion that can be drawn from the statistics displayed in **Figure 3** is that the global heat flux data set does not allow precise studies of the oceanic lithosphere. The very large data scatter is not due to measurement errors and will be now discussed further.

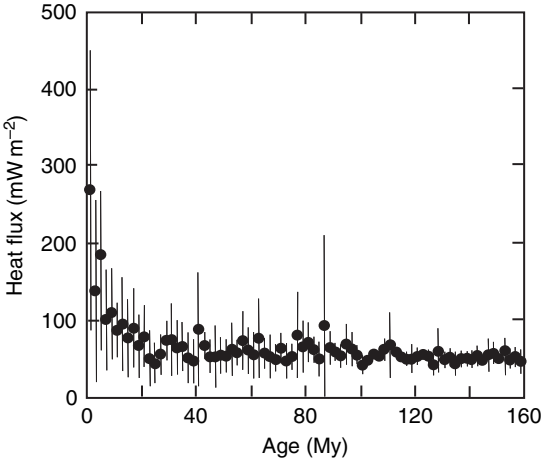

Figure 3 Oceanic heat flux data binned in 2 My intervals as a function of age, from the compilation by Stein and Stein (1992). Note the nonmonotonic variation of the mean heat flux and the extremely large data scatter at young ages.

6.05.3.2 Hydrothermal Circulation

Submarine observations of mid-ocean ridges have revealed spectacular plumes of hot aqueous solutions oozing out of the sea floor. Measurements on samples from Deep Sea Drilling Program (DSDP) and Ocean Drilling Program (ODP) boreholes and ophiolite massifs have shown that the oceanic crust is pervasively fractured and chemically altered. Mass balance calculations demonstrate that large volumes of fluid circulate through the crust, carrying large amounts of energy (e.g., Davis and Elderfield, 2004). *In situ* quantitative assessment of hydrothermal circulation can be achieved in two ways. One is to establish the energy budget of a vast area, such that it encompasses both downwellings and upwellings. For young ocean floor, upwellings carry hot fluids into the sea and a proper heat loss estimate can only be made by simultaneously measuring the discharge rate and the temperature anomaly (Ramondec *et al.*, 2006). With a thick sedimentary cover, upwellings are slowed down and become diffuse, and hence tend towards thermal equilibrium with the surrounding matrix. Testing that it is the case requires small-scale

temperature measurements at the water–sediment interface. The other method is to identify sites where hydrothermal convection is absent, but this is only possible on old sea floor.

6.05.3.3 Heat Flux Measurements Near Rift Zones

Several detailed surveys have led to a thorough understanding of the mass and heat balance of young oceanic basement and sedimentary cover. **Figure 4** (Davis *et al.*, 1999) shows a comparison between a heat flux profile on very young sea floor near the Juan de Fuca ridge and a cross-section showing the sediments thickness and basement depth. It was noted that the heat flux fluctuates on the scale of stations spacing (2 km), which implies that surveys with large stations spacing do not yield meaningful results. To emphasize the long wavelength trends, a 15 km running average was applied on the heat flux profile. This profile shows two distinct trends: near the basement outcrop, to the left, the heat flux increases with age and reaches a maximum value in excess of 400 mW m^{-2}; further away from the outcrop, the heat flux decreases with age. In the latter region, the total heat flux variation is large enough to allow comparison with theoretical models for the cooling of the ocean lithosphere.

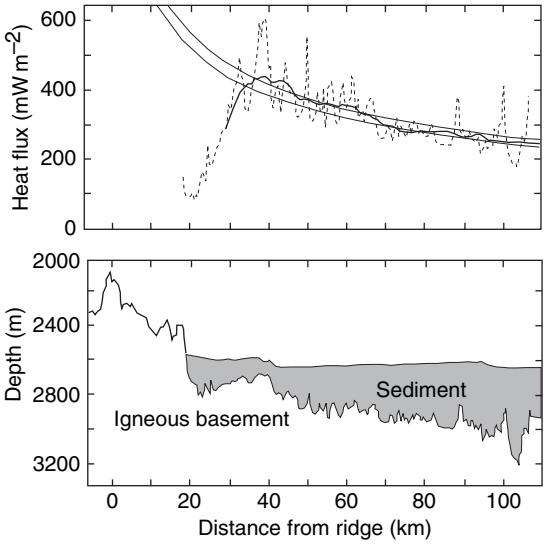

Figure 4 Top: Horizontal variation of heat flux away from Juan de Fuca ridge, from Davis *et al.* (1999). *Bottom*: Structure of young sea floor beneath the measurement sites, showing the lack of sedimentary cover at small distance from the ridge. The heat flux profile was obtained with a running average over 15 km windows. The two curves correspond to the half-space cooling model, such that $Q = C_Q \tau^{-1/2}$ with the two extreme values that have been proposed for $C_Q = 470$ and 510 mW m^{-2} My^{-1}.

Direct observation of the sea floor shows that the basement outcrop region is a zone of recharge and that, beneath the sedimentary cover, flow is dominantly horizontal. Because the basement surface is maintained approximately isothermal by vigorous convection, variations of heat flux seem mostly controlled by sediment thickness. But, focused discharge with very large heat flux values occurs at a few locations in association with basement topographic highs. Elsewhere, water flow is diffuse, such that it equilibrates with the sediments. Rates of flow deduced from chemical concentration gradients are consistent with theoretical hydrological calculations (Davis *et al.*, 1999). In order to evaluate the deep-seated heat flux, it is thus important to make measurements in a sufficiently large area with small sampling distance to filter out the effect of sediment thickness variability and of the ventilation areas.

6.05.3.4 Cooling Half-Space Model

Oceanic ridges are associated with mantle upwellings feeding plate-scale horizontal flow. Such flow occurs in a variety of settings and has been studied extensively. Flow is dominantly horizontal with negligible variations of horizontal velocity with depth. The large wavelengths of heat flow variations imply that heat transfer is dominantly vertical. In a two-dimensional (2-D) rectangular coordinate system, with x distance from the ridge and z depth from the sea floor, the temperature obeys the following equation:

$$\rho C_p \left(\frac{\partial T}{\partial t} + u \frac{\partial T}{\partial x} \right) = \frac{\partial}{\partial z} \left(k \frac{\partial T}{\partial z} \right) \qquad [4]$$

where u is the horizontal velocity, ρ is the density of the lithosphere, C_p the heat capacity, and k the thermal conductivity. We have neglected viscous heat dissipation and radiogenic heat production, which is very small in mantle rocks. Over the timescale of an oceanic plate, steady state can be assumed (i.e., the temperature remains constant at a fixed distance from the ridge). In steady state with constant thermal conductivity, the heat eqn [4] reduces to

$$\rho C_p u \frac{\partial T}{\partial x} = k \frac{\partial^2 T}{\partial z^2} \qquad [5]$$

For a constant spreading rate, the age τ is

$$\tau = x/u \quad [6]$$

which leads to

$$\frac{\partial T}{\partial \tau} = \kappa \frac{\partial^2 T}{\partial z^2} \quad [7]$$

where κ is thermal diffusivity. This is the 1-D heat diffusion equation, whose solution requires a set of initial and boundary conditions. The upper boundary condition and the initial condition can be specified with little error. The high efficiency of heat transport in the water column ensures that the sea floor surface is kept at a fixed temperature T_0 of about 4°C. The initial condition is set by a model for the ascent of hot material (Roberts, 1979). Over the horizontal scale of a mantle upwelling, one may neglect dissipation. Neglecting further lateral heat transfer, one can use solutions for isentropic pressure release (McKenzie and Bickle, 1988). For such an initial geotherm, temperature decreases with increasing height above the melting point. The total temperature drop depends on the starting mantle temperature, which sets the depth at which melting starts, and estimates for the heat of fusion, but never exceeds 200 K. This is much smaller than the difference ΔT between the surface and the starting temperature and it may be neglected in a first approximation. For uniform initial temperature $T_i = T_0 + \Delta T$, this model yields a heat flux proportional to $1/\sqrt{\tau}$:

$$Q = k\frac{\Delta T}{\sqrt{\pi\kappa\tau}} = C_Q \tau^{-1/2} \quad [8]$$

where $C_Q = k\Delta T/\sqrt{\pi\kappa}$ is a constant. As shown by Carslaw and Jaeger (1959) and Lister (1977), this simple age dependence also holds when physical properties are temperature dependent. In this model, by definition,

$$h_2 = \sqrt{\pi\kappa\tau} \quad [9]$$

The validity of this model can be assessed by going back to the Juan de Fuca heat flux data (**Figure 4**). The 15 km running average of heat flux measured over thick sediments fits the theoretical prediction beautifully. Three additional verifications may be made. The constant C_Q may be measured from the heat flux data. From well-known values of thermal conductivity and thermal diffusivity, we obtain an estimate for the mantle temperature $T_i = 1350$°C, which is very close to values deduced from the chemical composition of mid-ocean ridge basalts (Kinzler and Grove, 1992).

A second verification is provided by bathymetry data. Using an isostatic balance condition

$$\frac{dh}{dt} = \frac{\alpha}{C_p(\rho_m - \rho_w)} q(0, t) \quad [10]$$

where α is the volume thermal expansion coefficient, ρ_m the density of the mantle, and ρ_w the density of seawater. Thus,

$$h(\tau) = H_0 + C_h\sqrt{\tau} \quad [11]$$

with

$$C_h = \frac{2\alpha\rho_m\Delta T}{(\rho_m - \rho_w)}\sqrt{\frac{\kappa}{\pi}} \quad [12]$$

Bathymetry records the total cooling of the oceanic lithosphere since its formation at the mid-oceanic ridges. The bathymetry data are far less noisy than the heat flux data and fit extremely well the model predictions for oceanic lithosphere younger than ≈100 My (**Figure 5**). Again, the constant C_h can be calculated from the value of constant C_Q in the heat flow equation and checked against the observations. This was done by Davis and Lister (1974) following the theoretical analysis by Parker and Oldenburg (1973).

A third verification is possible thanks to geoid anomalies which decrease linearly with age. As before, the observed C_Q value can be used together with well-known values of physical properties to predict these anomalies, with excellent results (Haxby and Turcotte, 1978; Sandwell and Schubert, 1980).

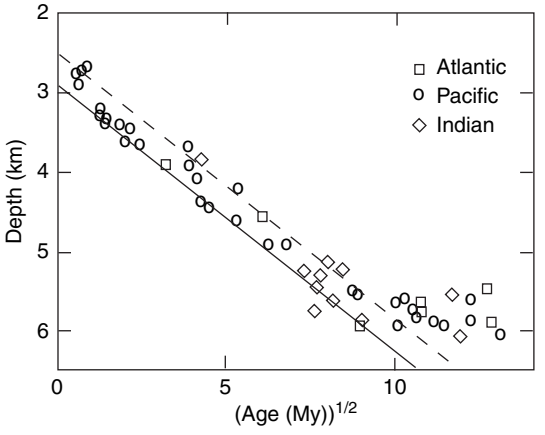

Figure 5 Depth to the sea floor basement as a function of the square root of age, from Carlson and Johnson (1994). These data correspond to DSDP holes and are not affected by uncertainties on sediment thickness. The dashed lines represent the two extreme linear relationships that are consistent with data.

The cooling model therefore accounts for all the observations on young sea floor and can be used to determine the mantle temperature. Should cooling proceed unhampered, the thermal boundary layer would thicken and reach a thickness of about 130 km by 180 My.

6.05.3.5 Old Ocean Basins: Flattening of the Heat Flow versus Age Curve

Heat flux data depart from eqn [8] on sea floor older than *c.* 100 My and tend to a constant value of $\approx$48 mW m^{-2} (**Figures 6** and 7). Depth to the ocean floor also departs from the theoretical predictions and tends to a constant value. These observations have been hotly debated and have important consequences that are discussed in the next section. Because heat flux data were scarce and subject to large experimental uncertainties, attention was focused on bathymetry. Depth values exhibit some scatter due to inaccurate estimates of sediment thickness and inherent basement roughness (Johnson and Carlson, 1992). Another issue was the influence of seamounts and large hot spot volcanic edifices, which obscure the behavior of 'normal' lithosphere, if such a thing exists (Heestand and Crough, 1981). Depth to the sea floor is indeed sensitive to the thermal structure of the whole upper mantle and to stresses at the base of the lithosphere, which depend on the dynamics of plate-scale convection (Davies, 1988). It turns out, therefore, that the flattening of the bathymetry does not allow straightforward conclusions.

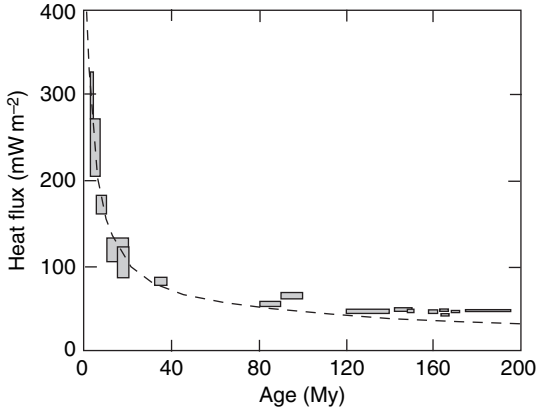

Figure 6 Reliable oceanic heat flux data as a function of age. The boxes represent the average heat flux in well-sedimented areas of the sea floor. The height of each box is the 90% confidence interval for the mean heat flux, and the width represents the age range, or uncertainty. The dashed line is the best-fit half-space cooling model. Note that heat flux data through old sea floor are systematically higher than the model predictions. Reproduced from Lister CRB, Sclater JG, Nagihara S, Davis EE, and Villinger H (1990) Heat flow maintained in ocean basins of great age – Investigations in the north-equatorial West Pacific. *Geophysical Journal International* 102: 603–630.

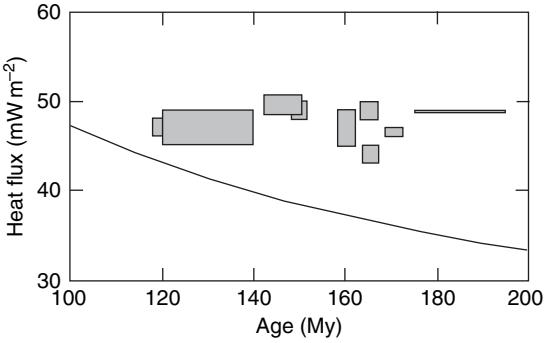

Figure 7 Closeup of the reliable oceanic heat flux data through sea floor older than 100 My. Within measurement uncertainty, these data suggest that heat flux is constant and about 48 mW m^{-2}. Reproduced from Lister CRB, Sclater JG, Nagihara S, Davis EE, and Villinger H (1990) Heat flow maintained in ocean basins of great age – Investigations in the north-equatorial West Pacific. *Geophysical Journal International* 102: 603–630.

Perhaps ironically, attention must go back to heat flux because it is sensitive neither to deep-mantle temperature anomalies nor to convective stresses. Over the limited age range of oceanic lithosphere, heat flow records shallow thermal processes within and just below the lithosphere (Davaille and Jaupart, 1994). This motivated detailed and accurate heat flux surveys through old sea floor (Lister *et al.*, 1990). New measurement techniques relying on longer temperature probes and *in-situ* conductivity measurements are affected by much smaller uncertainties (Becker and Davis, 2004). **Figure 7** shows reliable heat flux data including measurements specifically collected to detect age-related variations if there were any. It is clear that heat flux departs from the $1/\sqrt{\tau}$ behavior and exhibits no detectable variation at ages larger than about 120 My. This indicates that heat is supplied to the lithosphere from below.

6.05.3.6 Modified Thermal Model for the Oceanic Lithosphere

Data on old sea floor indicate that heat is brought into the lithosphere from below, which has led to the 'plate' model such that a boundary condition is specified at some fixed depth (the base of the plate). **Figure 8** illustrates the relationships between the thermal

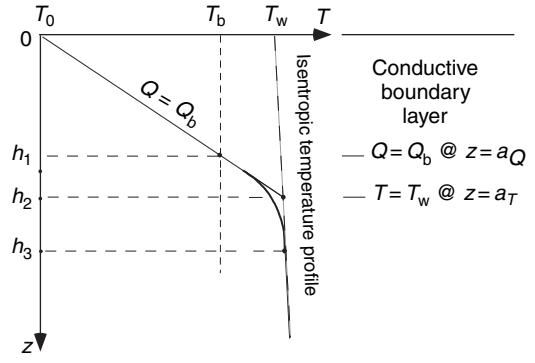

Figure 8 Left: Schematic structure of the thermal boundary layer at the top of the Earth's convecting mantle. *Right*: Two simple plate models and their relationships to the true boundary layer structure. The fixed temperature model corresponds to thickness h_2 and to temperature T_w. The fixed heat flux model corresponds to thickness h_1 and to temperature T_b.

boundary layer structure and the plate model characteristics. The original plate model of McKenzie (1967) is such that the plate is initially at a fixed temperature ΔT_T, the surface is maintained at $T = 0$ and the base of the plate at depth a_T is maintained at ΔT_T. With reference to **Figure 1**, one has $a_T = h_2$, showing that the fixed temperature model does not specify the thickness of the unstable boundary layer at the base of the lithosphere.

Assuming for simplicity that physical properties are constant, an important point to which we shall return, temperature within the plate obeys the following equation:

$$T(z,t) = \Delta T_T \left(\frac{z}{a_T} + \frac{2}{\pi} \sum_{n=1}^{\infty} \frac{1}{n} \sin\left(\frac{n\pi z}{a_T}\right) \times \exp\left(\frac{-n^2\pi^2\kappa t}{a_T^2}\right)\right) \quad [13]$$

which defines a characteristic time

$$\tau_T = \frac{a_T^2}{\kappa} \quad [14]$$

For $t \gg \tau_T$, the series can be approximated by its leading term, as follows:

$$T(z,t) = \Delta T_T \left(\frac{z}{a_T} + \frac{2}{\pi} \sin\left(\frac{\pi z}{a_T}\right) \times \exp\left(-\frac{\pi^2\kappa t}{a_T^2}\right)\right) \quad [15]$$

which shows straightforward relaxation behavior. Surface heat flux and depth to the sea floor are readily calculated from this solution and are in good overall agreement with the observations (Parsons and Sclater, 1977). There are small systematic differences between model predictions and observations, however, indicating that the model is only an approximation (Johnson and Carlson, 1992). Depending on the data set and on model specifications (such as temperature-dependent physical properties), the analysis provides estimates of $\approx$100 km and 1300°C for a_T and ΔT, respectively (**Table 2**). As in the case of the half-space model, the model can be tested against direct petrological estimates of the mantle temperature (McKenzie and Bickle, 1988; Kinzler and Grove, 1992). This test invalidates the widely used model of Stein and Stein (1992), which requires $\Delta T = 1450$°C.

An alternative plate model corresponds to the fixed-flux boundary condition. In this case, the plate is initially at temperature ΔT_Q and fixed flux $k\Delta T_Q / a_Q$ is maintained at the base a_Q, which is in fact h_1 (**Figure 8**). The solution is

$$T(z,t) = \frac{\Delta T_Q z}{a_Q} + \frac{8\Delta T_Q}{\pi^2} \sum_{n=0}^{\infty} \frac{1}{(2n+1)^2} \times \cos\left(\frac{(2n+1)\pi z}{2a_Q}\right) \times \exp\left(\frac{-(2n+1)^2\pi^2\kappa t}{4a_Q^2}\right) \quad [16]$$

where the temperature difference ΔT_Q corresponds to steady state with basal heat flux Q_b:

$$\Delta T_Q = \frac{Q_b a_Q}{k} \quad [17]$$

and where the characteristic relaxation time is

$$\tau_Q = 4\frac{a_Q^2}{\kappa} \quad [18]$$

Table 2 Parameter values for the oceanic plate model

ΔT (°C)	a (km)	Method	Reference
1333	125	Constant properties – fixed T	Parsons and Sclater (1977)
1450	95	Constant properties – fixed T	Stein and Stein (1991)
1350	118	T-dependent properties – fixed Q at variable depth[a]	Doin and Fleitout (1996)
1315	106	T-dependent properties – fixed T	McKenzie *et al.* (2005)

[a]In this model, heat flux is fixed at the base of the growing thermal boundary layer.

With this solution, the leading term in the series expansion for the age dependence of heat flux and bathymetry exhibits the same type of relaxation than for a fixed basal temperature but with a different value for the characteristic relaxation time. A fit to the data forces the two relaxation times to take the same value of about 80 My, the age at which the subsidence departs from boundary layer cooling subsidence. This leads to

$$a_Q = \frac{a_T}{2} \approx 50\,\text{km} \qquad [19]$$

This model does not specify the characteristics of the unstable boundary layer. With reference to **Figure 2**, one has $a_T = b_2$ and $a_Q = b_1$. Thus, the solutions for the two plate models are consistent with the fundamental inequality $b_2 > b_1$. The estimate for b_1 may be compared to the thickness of depleted mantle, which depends on the well-mixed mantle potential temperature (T_w). For $T_w \approx 1300°C$, this is ≈60 km. Accounting for the various uncertainties involved, the two estimates may be considered in satisfactory agreement.

The point of this discussion is not to dwell on precision, which would require more complex calculations with temperature-dependent properties, but to show how to interpret thickness estimates deduced from thermal models. It makes it clear, for example, that the fixed temperature model cannot be used to determine the thickness of melt-depleted mantle. This model, however, provides temperature estimates for the whole oceanic boundary layer. **Figure 9** shows the most recent improvement of this model by McKenzie *et al.* (2005), which accounts for temperature-dependent physical properties.

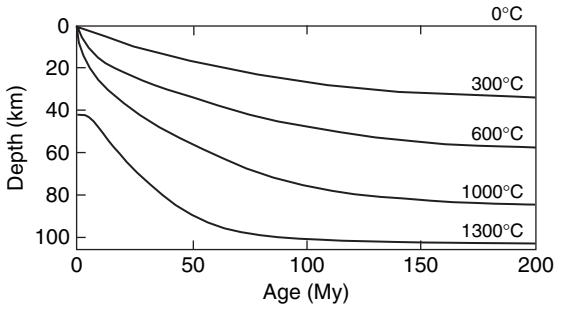

Figure 9 Isotherms in the oceanic lithosphere from the plate model of McKenzie *et al.* (2005). Earthquake hypocenters are confined to shallow regions above the 600°C isotherm.

From a physical standpoint, the fixed temperature and fixed heat flux models must both be considered as crude simplifications. The former requires a specific time variation of heat flux at the base of the lithosphere, which may not be consistent with true mantle dynamics. The latter model requires that heat is brought into the lithosphere at small ages. More complex models have a fixed heat flux brought to the base of a growing thermal boundary layer (Doin and Fleitout, 1996), at which point it is perhaps best to turn to full numerical simulations (Dumoulin *et al.*, 2001; Huang and Zhong, 2005).

6.05.3.7 Variations of Lithospheric Thermal Structure due to Factors Other Than Age

6.05.3.7.1 Large-scale variations of mantle temperature

The chemical composition of mid-ocean ridge basalts varies within a restricted range, but these variations are highly significant (Klein and Langmuir, 1987) because they require that the mantle temperature is not uniform along a ridge axis. Detailed petrological studies yield a range of 1300–1450°C for the source temperature (Kinzler and Grove, 1992). This range does not correspond to experimental errors, but to compositional variations among mid-ocean basalts which are due to variations in source temperature. Depending on which scale these variations occur, their causes and consequences differ strongly. Small-scale heterogeneities would be of local significance only and would have no effect on geophysical observables. Large-scale heterogeneities would indicate the existence of large mantle domains and would imply variations in plate temperatures and physical properties.

Heat flux data allow accurate determination of the heat flux cooling constant, C_Q, between 470 and 510, corresponding to an uncertainty of only ≈4%. In terms of mantle temperature, assuming no uncertainty on the thermal properties entering the expression for C_Q, this corresponds to an uncertainty for T_i of ≈±60°C. This is compatible with the petrological estimates but does not allow an independent constraint. Bathymetry data exhibit large-scale trends with along-strike variations of ridge topography as well as of subsidence rate (Marty and Cazenave, 1989). With a modified plate model, one may estimate that the mantle temperature varies by about ±100°C (Lago *et al.*, 1990). Such variations occur on a large scale and may be traced from the ridge to old sea floor (Humler *et al.*, 1999).

6.05.3.7.2 Hot spots

Hot spots are associated with spectacular swells on the sea floor (Crough, 1983). Debate has been on whether mantle plumes are involved and on the extent of lithospheric thinning. Several mechanisms can be invoked for a bathymetric swell, involving heating of lithospheric material or a normal stress applied to the base of the lithosphere by an active mantle upwelling (i.e., a dynamic stress) or by ponded buoyant (hot) plume material (Jurine *et al.*, 2005).

The search for heat flux anomalies over hot spot swells has led to mixed results. Courtney and White (1986) found a weak anomaly over Cape Verde. Bonneville *et al.* (1997) had to resort to closely spaced measurements to detect a small anomaly of about 8 mW m^{-2} over the Reunion hot spot track. A global analysis shows that swells are associated with above-normal heat flux values (Stein, 1995). Without lithosphere thinning, it would take about 100 My for a basal thermal perturbation to be detectable in surface heat flux data. No heat flux anomaly is above the error level along the Hawaiian hot spot track, probably due to hydrothermal convection within the sedimentary moat surrounding the island (Von Herzen *et al.*, 1989; Harris *et al.*, 2000). However, a recent seismic study by Li *et al.* (2004) indicates thinning by ≈50 km of the lithosphere beneath the island of Kauai.

The data indicate modifications of lithospheric thickness and thermal structure above mantle plumes, as expected on physical grounds (Moore *et al.*, 1999; Jurine *et al.*, 2005). Such modifications, however, depend on plume strength and lithosphere thickness and must be evaluated on a case by case basis.

6.05.3.8 Summary

At small ages, heat flux data are noisy and their small-scale variations are not sensitive to deep thermal conditions. For ages less than 100 My, heat flux data are consistent with conductive cooling of the oceanic lithosphere and yield an estimate of the mantle temperature. The deepening of bathymetry with age provides a direct measure of the time integrated cooling of the lithosphere. The observed bathymetry versus age relationship is the strongest supporting evidence for the cooling model. For old ages, plate models relying on specific choices for the basal boundary condition must be considered as approximate and they cannot specify how the lithosphere thickness stabilizes to a constant value. Heat flux data provide some insight into convective processes because they specify the rate at which heat is brought to the base of the lithosphere. Determination of plate thickness from a thermal model is subject to some ambiguity because it depends on assumed boundary conditions.

6.05.4 Continental Lithosphere in Steady State

6.05.4.1 Vertical Temperature Distribution

There is now no doubt that the continental lithosphere is much thicker than its oceanic counterpart. The choice of a boundary condition at the base of the lithosphere is important when considering the transient regime and the return to equilibrium. For a 200 km thick lithosphere with constant temperature at its base, the thermal relaxation time is ≈300 My. As shown above, it would be four times as long for a constant heat flow boundary condition. Gass *et al.* (1978) and Jaupart *et al.* (1998) have also pointed out that for lateral changes in basal heat flux to reach the surface, they must remain immobile relative to the lithosphere for more than 1 Gy. Basal boundary conditions varying on a timescale <500 My have little or no effect on surface heat flux. A thick lithosphere introduces two additional complexities. One is that even very small concentrations of radioelements in the lithospheric mantle may account for a non-negligible fraction of the total heat flow. Another is that the surface heat flux cannot be in equilibrium with the present heat production in the lithospheric mantle (Michaut and Jaupart, 2004).

In the crust, the progressive rundown of radioactivity is slow compared to thermal equilibration time and steady state may be assumed in many situations. Because heat production varies at all scales, the approach must depend on the scale of the study (Jaupart and Mareschal, 2003; Mareschal and Jaupart, 2004). Deep horizontal variations of heat production (and also of basal heat flux) are smoothed out by diffusion. Conventional wisdom from potential theory is that short-wavelength variations are associated with shallow sources whereas long-wavelength ones might be due to deep sources. For heat flow, the former is certainly true but not the latter: crustal sources reflect the surface geology which follows a long-wavelength pattern. Starting from the surface, downward continuation is unstable for small wavelengths. In practice, one must use an

averaging window 100 km wide for crustal temperatures and 500 km wide for the deep lithosphere.

With a reliable model for the vertical variation of the horizontally averaged heat production, $A(z)$, the surface heat flux Q_0 can be written as

$$Q_0 = Q_M + \int_0^{z_m} A(z')\mathrm{d}z' \qquad [20]$$

where z_m is depth to Moho. Note that one may not assume that Q_b, the heat flux at the base of the lithosphere, is equal to Q_M, the heat flux at the Moho, because of long thermal transients and heat production in the lithospheric mantle. Such issues will be discussed separately. In steady state, vertical temperature profiles are obtained by integration:

$$k(T)\frac{\mathrm{d}T}{\mathrm{d}z} = Q_0 - \int_0^z A(z')\mathrm{d}z' \qquad [21]$$

where $k(T)$ is the temperature-dependent thermal conductivity. In practice, the function $A(z)$ is not well known but one may obtain constraints on the Moho heat flow, as will be explained below. As a first approximation, one may neglect heat production in the lithospheric mantle. Specifying the values of heat flux at the surface and at the Moho then sets the total amount of crustal heat production, which leaves only one unknown: the vertical variation of heat production in the crust.

Figures 10–12 illustrate the effects of changing the three main variables: the surface heat flux, the Moho heat flux, and the vertical distribution of crustal heat production. For accurate predictions, calculations must account for temperature-dependent conductivity (see Appendix 4). For a stratified crust with an enriched upper layer and a fixed Moho heat flux, increasing the surface heat flux from 40 to 90 mW m^{-2} leads to small temperature differences in the mantle (≈100 K). Temperatures are more sensitive to changes of the vertical distribution of heat production (**Figure 11**). As discussed below, current estimates for the Moho heat flux beneath cratons range from 12 to 18 mW m^{-2}. This range of variations leads to large differences in temperatures in the lowermost lithosphere (≈250°C).

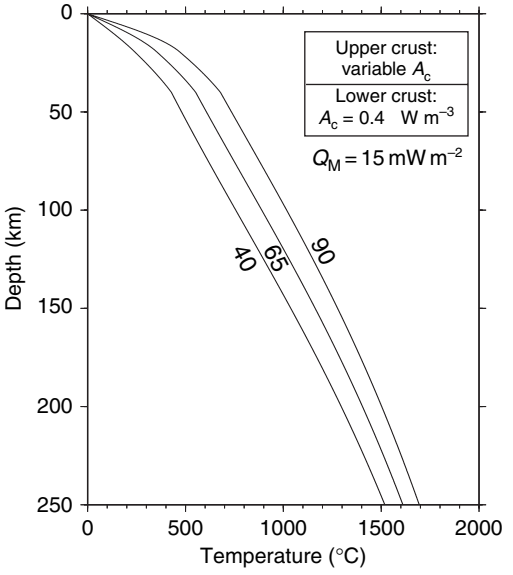

Figure 10 Three continental geotherms calculated for surface heat flux = 40, 65, and 90 mW m^{-2}. Calculations are made with temperature-dependent conductivity (see Appendix) and for the same Moho heat flow of 15 mW m^{-2}. Crustal heat production is assumed to be distributed in two layers of equal thickness with a fixed value of 0.4 μW m^{-3} for heat production in the lower crust. With such models, changing the surface heat flux by 25 mW m^{-2} leads to changes of ≈110°C and 100°C for temperatures at the Moho and at 200 km depth.

6.05.4.2 Crustal Heat Production

It is now clear that there is no 'universal' law that relates crustal heat production to surface heat flux, or that allows the heat flux and heat production to be determined from crustal age. In principle, the distribution of radiogenic heat production could be obtained by sampling all representative rocks in a geological province. This is rarely feasible in practice because of a lack of samples from the lower crust (Jaupart and Mareschal, 2003). The vagaries of geochemical studies are seldom consistent with those of heat flow studies, implying that one must deal with poorly matched data sets. For these reasons, some authors have searched for shortcuts and have tried to derive the crustal heat production directly from the heat flux data.

Early work on continental heat flux revealed, within certain provinces, a linear relationship between the local values of heat flux Q and heat production A_0 (Birch *et al.*, 1968):

$$Q = Q_r + A_0 D \qquad [22]$$

The slope D, which has dimension of length and is usually ≈10 km, is related to the thickness of a surficial heat producing layer. Q_r is called the reduced heat flux. The region where the relationship holds defines a heat flux province characterized by D and Q_r. Within the relatively large errors in both heat flux

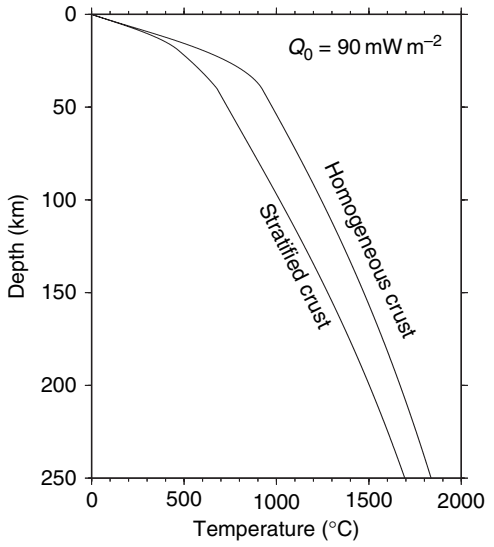

Figure 11 Two continental geotherms for the same heat flux value of 90 mW m^{-2} and two different vertical distributions of crustal heat production. Calculations are made with temperature-dependent conductivity (see text) and for the same Moho heat flow of 15 mW m^{-2}. One curve corresponds to a stratified continental crust, as in **Figure 10**, and the other to a homogeneous crust. Changing the vertical distribution of heat production leads to changes of ≈220°C and 140°C for temperatures at the Moho and at 200 km depth.

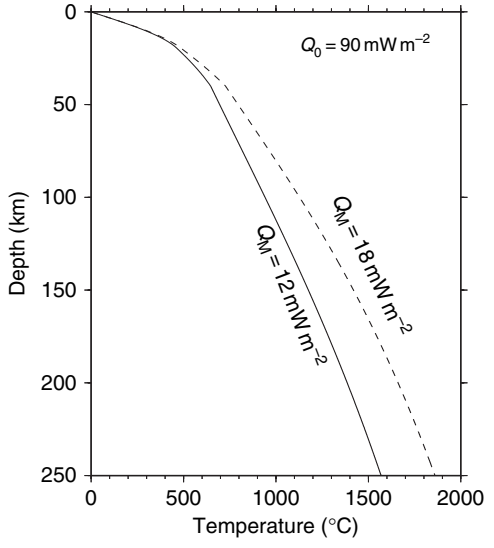

Figure 12 Two continental geotherms for the same heat flux value of 90 mW m^{-2} and two different values of the Moho heat flux (12 and 18 mW m^{-2}). Calculations are made with temperature-dependent conductivity (see text) and for the same stratified crustal model as in **Figure 10**. Changing the Moho heat flux leads to changes of ≈100°C and 260°C for temperatures at the Moho and at 200 km depth.

and heat production values, several such provinces were defined, including the Sierra Nevada and the Basin and Range, which are not in steady state. Among the many heat source distributions that fit this relationship, the exponentially decreasing one, $A(z) = A_0 \exp(-z/D)$, was favored because it is independent of the erosion level (Lachenbruch, 1970). With this model, the total heat production in the crust is $\approx A_0 \times D$ and $Q_M \approx Q_r$ if D is less than 10 km. This (and other) simple models based on the linear relationship imply that the vertical distribution of heat production can be described by a single universal function with well-defined parameters within each province. If this concept was verified, it would be possible to infer the vertical distribution of heat production as well as the mantle heat flux directly from surface heat flux. For instance, Artemieva and Mooney (2001) have followed this approach to determine the thickness and temperature in the continental lithosphere on a worldwide scale from the global heat flux compilation.

With the large data sets now available, it is clear that the concept of a universal vertical heat production distribution is not valid. The correlation between local values of surface heat flux and heat production only holds over exposed plutons very enriched in radioactive elements. Over other rock types, it is weak at best, as demonstrated by data from large Precambrian provinces of India (Roy and Rao, 2000), Canada (Mareschal *et al.*, 1999), and South Africa (Jones, 1987, 1988). Theory shows that, for the rather small wavelengths involved, surface heat flux is only sensitive to shallow heat-production contrasts (Jaupart, 1983a). In fact, the linear relationship is an artifact because horizontal heat transport smoothes out deep differences in heat production rates. Values of D are not related to other physical dimensions in a geological province, such as pluton thickness, and are related to the horizontal correlation distance of heat production (Jaupart, 1983b; Vasseur and Singh, 1986; Nielsen, 1987). One unfortunate consequence is that the reduced heat flux is not the mantle heat flux, but the heat flux at some intermediate crustal depth. Thus, one cannot get around the problem of estimating heat production in the mid and lower crust.

Following a related approach, Pollack and Chapman (1977a, 1977b) noted a correlation between the reduced heat flux and the average heat flux $\bar{Q}$ in a few geological provinces. They added estimates of lower crustal heat production and obtained a model

in which the mantle and surface heat fluxes are nearly proportional to each other. This relationship is not valid at short spatial scales by construction and is not consistent with data from several well-sampled regions, as shown below.

Sampling of different structural levels in the crust, studies of lower crustal xenoliths, and studies in very deep boreholes have given us much needed estimates of the vertical distribution of heat generation. Samples from the lower crust show that heat production is not negligible. Xenoliths lead to a global average heat production of $0.28\,\mu W\,m^{-3}$ (Rudnick and Fountain, 1995) while exposed rocks from lower crustal levels yield $0.4–0.5\,\mu W\,m^{-3}$ (**Figure 13**). These values are much too high to be consistent with an exponential decrease of heat sources. Studies of exposed crustal sections suggest a general trend of decreasing heat production with depth, but this trend is not a monotonic function (Ashwal *et al.*, 1987; Fountain *et al.*, 1987; Ketcham, 1996). Even for the Sierra Nevada batholith, where the exponential model had initially been proposed, a recent compilation has shown that the heat production does not decrease exponentially with depth (Brady *et al.*, 2006). In the Sierra Nevada, heat production first increases, then decreases and remains constant in the lower crust beneath 15 km. Measurements in very deep boreholes (Kola, KTB) have shown that the concentration of heat sources does not systematically decrease with depth. At Kola, the Proterozoic supracrustal rocks (above 4 km) have much lower heat production ($0.4\,\mu W\,m^{-3}$) than the Archean basement ($1.47\,\mu W\,m^{-3}$) (Kremenentsky *et al.*, 1989). At KTB, heat production decreases with depth at shallow levels, reaches a minimum between 3 and 8 km, and increases again in the deepest part of the borehole.

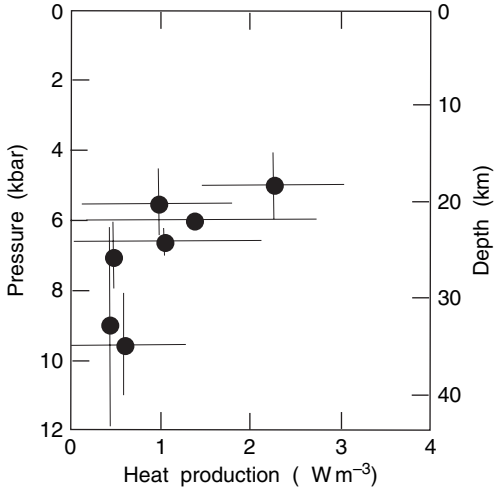

Figure 13 Radiogenic heat production in granulite-facies rocks from the Baltic and Canadian shields as a function of peak metamorphic pressure. Note that heat production does not drop below $0.4\,\mu W\,m^{-3}$. Reproduced from Joeleht TH and Kukkonen IT (1998) Thermal properties of granulite facies rocks in the Precambrian basement of Finland and Estonia. *Tectonophysics.* 291: 195–203.

These results may perhaps seem obvious to geologists trained to deal with the complexities of crustal structure and processes. A universal function describing the vertical distribution of heat production requires a ubiquitous mechanism affecting all crustal rocks in the same manner everywhere. A natural candidate would be fluid redistribution accompanying metamorphic reactions, but we know that it does not affect uranium and thorium (Bingen *et al.*, 1996; Bea and Montero, 1999). It is now clear that heat production in the lower crust depends mostly on prior geological history. One cannot expect that tectonic and magmatic processes somehow manage to redistribute heat production in a systematic fashion on a scale of a few to a few tens of kilometers.

As shown above, one key step is to derive reliable average values for both the surface and Moho heat fluxes. Their difference yields the total amount of heat produced in the crust. Adding an estimate of the average heat production at the surface, one can further obtain a measure of its vertical variations. For that reason, Perry *et al.* (2006) introduced a differentiation index:

$$D_I = \frac{A_0}{< A >} \qquad [23]$$

where A_0 is the surface heat production and $<A>$ is the mean crustal heat production. If Moho heat flux is Q_M and crustal thickness H,

$$D_I = \frac{A_0 H}{Q_0 - Q_M} \qquad [24]$$

How to obtain estimates of the Moho heat flux is discussed in the next section. Crustal stabilization requires vertical differentiation of the radioelements. This operates as a self-regulating system: high heat production with uniform vertical distribution gives rise to elevated temperatures favoring melting in the lower crust and differentiation (Sandiford and McLaren, 2002). One can thus expect the differentiation index to be high when average crustal heat production and surface heat flux are high; for example, $D_I \approx 3$ and 1 for the Phanerozoic Appalachians and Grenville Provinces, North America, respectively (**Figure 14**). It is expected that crustal differentiation

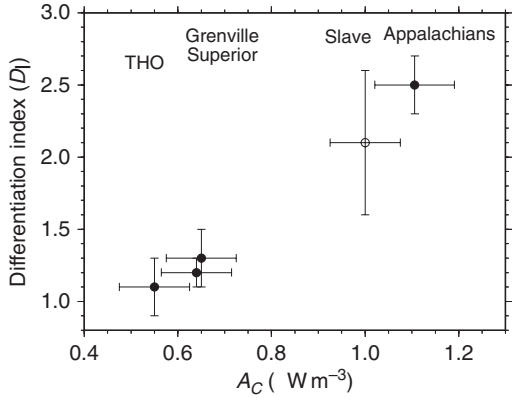

Figure 14 Crustal differentiation index D_I as a function of average crustal heat production in five large geological provinces of North America. Reproduced from Perry HKC, Jaupart C, Mareschal JC, and Bienfait G (2006) Crustal heat production in the Superior Province, Canadian Shield, and in North America inferred from heat flow data. *Journal of Geophysical Research* 111, B04401 (doi:10.1029/2005JB003,893).

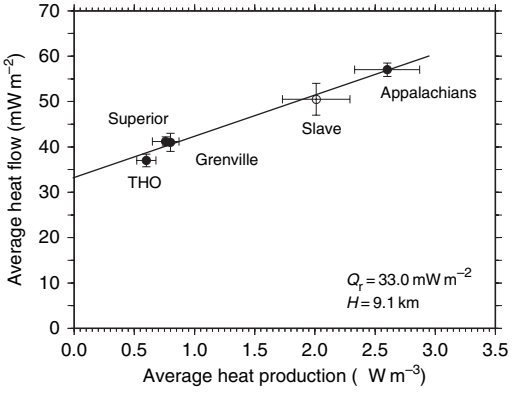

Figure 15 Relationship between the average values of heat flow and surface heat production for five large geological provinces of North America. Reproduced from Perry HKC, Jaupart C, Mareschal JC, and Bienfait G (2006) Crustal heat production in the Superior Province, Canadian Shield, and in North America inferred from heat flow data. *Journal of Geophysical Research* 111, B04401 (doi:10.1029/2005JB003,893).

should lead to $D_I > 1$. This is not always the case, because the rocks exposed at the surface can be brought up by other processes than magmatic differentiation. For instance, in the Flin Flon volcanic belt of the Proterozoic Trans-Hudson Orogen (THO), North America, $D_I \approx 0.4$. A similar value is obtained at the Kola superdeep hole. In both cases, the Proterozoic supracrustal rocks were tectonically transported over a more radiogenic Archean basement.

6.05.4.3 Mantle Heat Flux

When the lithosphere is thick, variations in basal heat flux are unlikely to be reflected in the surface heat flux. Indeed, except for very long wavelengths, any basal heat flux variation of amplitude ΔQ_b is attenuated when upward continued to the surface (Mareschal and Jaupart, 2004):

$$\Delta Q_0 = \frac{\Delta Q_b}{\cosh(2\pi L/\lambda)} \qquad [25]$$

where L is the lithosphere thickness and λ the wavelength of the variation. As mentioned above, ΔQ_b must be understood as a time average over >500 My. Likewise, for wavelengths less than 500 km, horizontal temperature variations in the lithosphere induced by changes in the basal heat flux would be larger than the ±200 K inferred from xenoliths and seismic data. Mareschal and Jaupart (2004) concluded that variations in the basal heat flux accounts for less than ±2 mW m^{-2} of the surface heat flux variations that is, they are comparable to the uncertainty on the heat flux determination. As shown by **Figure 15**, variations in crustal heat production account for the variability of surface heat flux in all the major provinces of North America (Pinet *et al.*, 1991; Jaupart *et al.*, 1998; Lewis *et al.*, 2003). Such a correlation leaves little room for variations of the mantle heat flux, which is an independent variable. The sharpness of the variations in surface heat flux between provinces also requires that they originate in the crust. For example, the transition between the Grenville and the Appalachians takes place over less than 50 km (Mareschal *et al.*, 2000).

Values of the mantle heat flux may be obtained using two independent methods. In the Abitibi subprovince of the Archean Superior Province, Canada, xenolith suites from the Kirkland Lake kimberlite pipe yield temperatures and pressures corresponding to a wide depth range. The temperature estimates are lower than temperatures in the convecting mantle at depths less than 200 km (**Figure 16**). With an estimate of thermal conductivity in the mantle, Rudnick and Nyblade (1999) found a best-fit Moho heat flux ≈18 mW m^{-2}, within a range of 17–25 mW m^{-2}. Another method relies on the variations of heat flux and crustal structure combined with heat-production data for the various rock types. For the same Abitibi area, Guillou *et al.* (1994) incorporated constraints from seismic and gravity data to arrive at a range of

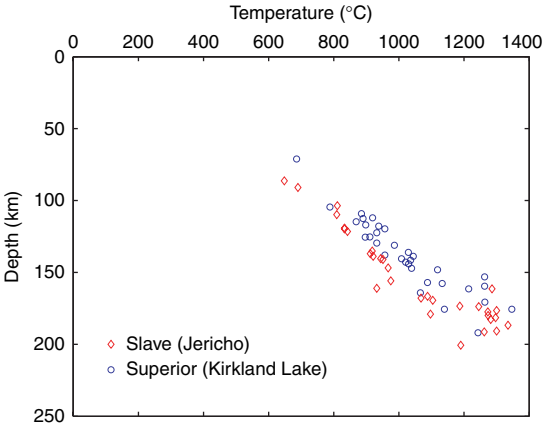

Figure 16 Temperature and pressure values for equilibrium mineral assemblages in xenoliths from two kimberlite pipes in the Canadian Shield. Data taken from Rudnick RL and Nyblade AA (1999) The thickness of Archean lithosphere: Constraints from xenolith thermobarometry and surface heat flow. In: Fei Y, Bertka CM, and Mysen BO (eds.) *Mantle Petrology; Field Observations and High Pressure Experimentation: A Tribute to Francis R. (Joe) Boyd,* pp. 3-11. Houston TX: Geochemical Society.

7–15 mW m^{-2} for Q_M. These two independent estimates can be combined to reduce the uncertainty: values lower than 15 mW m^{-2} would not be consistent with the xenolith data and values higher than 18 mW m^{-2} would not be compatible with heat flux and heat-production data.

Similar agreement between these two methods has been obtained in other provinces, in South Africa for example. There, the deep crustal section exposed in the Vredefort structure allowed an estimate of 18 mW m^{-2} for the Moho heat flux in the Kaapvaal craton (Nicolaysen *et al.*, 1981), very close to the value deduced from xenolith (P,T) data (Rudnick and Nyblade, 1999).

There are now enough data to directly assess whether the mantle heat flux varies as a function of age or as a function of distance across a craton. In the Canadian Shield, xenoliths samples from the Jericho kimberlite pipe of the Archean Slave Province, more than 2000 km northwest of the Abitibi, give a best-fitting value of 15 mW m^{-2} for mantle heat flow value within a range between 12 and 24 mW m^{-2} (Russell *et al.*, 2001). This wide range is due to the data interpretation technique, which leaves the temperature dependence of thermal conductivity as a variable to be solved for. In the Lac de Gras kimberlite pipes, which also belong to the Slave Province, surface heat flux data are available and allow tighter constraints of 12–15 mW m^{-2} for Q_M (Mareschal *et al.*, 2004). Crustal models lead to mantle heat flow values of 10–15 mW m^{-2} for the *c.* 1.8 Ga THO (Rolandone *et al.*, 2002) and for the *c.* 1.0 Ga Grenville Province (Pinet *et al.*, 1991).

Lower and upper bounds on Q_M can be derived using other arguments. Rolandone *et al.* (2002) calculated lower crustal temperatures when different provinces of the Canadian Shield stabilized, which depend on the crustal heat production. Requiring that temperatures were below melting, they found that Q_M could not be less than about 12 mW m^{-2}. Upper bounds on the mantle heat flow can be derived from the lowest heat flux measured in the Shield.

Heat flux values of 22–23 mW m^{-2} are found in the center of the Shield, in the THO (Mareschal *et al.*, 1999) and at the eastern edge of the Shield, at Voisey Bay, Labrador (Mareschal *et al.*, 2000). Because of horizontal heat diffusion, such values include the contribution of crustal heat production averaged over large volumes (Mareschal and Jaupart, 2004). Using a lower bound of 0.2 μW m^{-3} on crustal heat production leads to a refined upper bound of 15 mW m^{-2} for Q_M.

Using these constraints simultaneously, the mantle heat flow beneath the Canadian Shield cannot vary by more than ±3 mW m^{-2} around a value of 15 mW m^{-2}, implying that variations of lithosphere thickness do not exceed ≈±50 km.

Similar results have been obtained in other continents and are listed in **Table 3**. In the Baltic and in the Siberian shields, the lowest regional average heat flux values are 15 and 18 mW m^{-2}, respectively (**Table 4** and references therein). Such measurements provide upper limits on mantle heat flow that are even lower than in Canada.

6.05.4.4 Regional Variations of Heat Flow and Lithospheric Temperatures

Table 3 shows the average heat flux from different provinces grouped according to age. The trend of decreasing heat flux with age is weak at best and shows remarkable exceptions. In North America, variations of heat flux can be accounted for by changes of crustal heat production, as explained above. For stable continents, the very wide range of average heat fluxes within each age group (Archean, 36–50 mW m^{-2}; Proterozoic, 36–94 mW m^{-2}; Paleozoic: 30–57 mW m^{-2}) implies that age is not a proxy for heat flux. This range suggests that surface heat flux reflects the structure and composition of the continental crust, which vary due to the

Table 3 Mean heat flux and heat production in major provinces

	$\langle Q \rangle$[a] (mW m^{-2})	N_Q[c]	$\langle A \rangle$[a]	σ_A[b] (μW m^{-3})	N_A[c]	References
Archean						
Dharwar (India)	36 ± 2.1	8				Roy and Rao (2000)
Kaapvaal basement[d] (S. Africa)	44	81	1.8	—		Ballard *et al.* (1987), Jones (1988)
Zimbabwe (S. Africa)	47 ± 3.5	10	1.34	—	—	Jones (1987)
Yilgarn (Australia)	39 ± 1.5	23	3.3	—	540	Cull (1991), Jaupart and Mareschal (2003)
Superior (N. America)	41 ± 0.9	70	0.72	0.73	64	Mareschal *et al.* (2000)
Slave (N. America)	50 ± 3.5	3	2.3	1.0	20	Mareschal *et al.* (2004)
Wyoming (N. America)	48.3 ± 5.7	6	3.1	2.1	6	Decker *et al.* (1980)
Total Archean[e]	41 ± 0.8	188				Nyblade and Pollack (1993)
Proterozoic						
Aravalli (India)	68 ± 4.9	7				Roy and Rao (2000)
Namaqua (S. Africa)	61 ± 2.5	20	2.3		10	Jones (1987)
Gawler (Australia)	94 ± 3	6	3.6	—	90	Cull (1991), Jaupart and Mareschal (2003)
Sao Francisco craton (Brazil)	42 ± 5	3	1.5	0.6	3	Vitorello *et al.* (1980)
Braziliane mobile belt (Brazil)	55 ± 5	8	1.7	1.2	5	Vitorello *et al.* (1980)
Ukrainian Shield	36 ± 2.4	12	0.9	0.2	7	Kutas (1984)
Trans-Hudson (N. America)	42 ± 2.0	49	0.73	0.50	47	Rolandone *et al.* (2002)
Wopmay (N. America)	90 ± 1.0	12	4.8	1.0	20	Lewis *et al.* (2003)
Grenville (N. America)	41 ± 2.0	30	0.80	[f]	17	Mareschal *et al.* (2000)
Total Proterozoic[e]	48 ± 0.8	675				Nyblade and Pollack (1993)
Paleozoic						
Appalachians (N. America)	57 ± 1.5	79	2.6	1.9	50	Jaupart and Mareschal (1999)
Basement United Kingdon	49 ± 4.4	6	1.3	0.5	6	Lee *et al.* (1987)
Urals	30 ± 2	40				Kukkonen *et al.* (1997)
Total Paleozoic[e]	58.3 ± 0.5	2213				Pollack *et al.* (1993)

[a] Mean ± one standard error.
[b] Standard deviation on the distribution.
[c] Number of sites.
[d] After removing the contribution of the sediments.
[e] Total in the compilation by Nyblade and Pollack (1993) excluding the more recent measurements included here.
[f] Area-weighted average value.

Table 4 Regional variations of the heat flux in different cratons

	Minimum	Maximum
	(mW m^{-2})	
Superior Province	22	48
Trans-Hudson Orogen	22	50
Australia	34	54
Baltic Shield	15	39
Siberian Shield	18	46

Minimum and maximum values obtained by averaging over 200 km × 200 km windows.

competing mechanisms of crustal extraction from the mantle and crustal recycling. In the Proterozoic provinces, high heat flux and crustal heat production (e.g., Wopmay Orogen, Thompson Belt in the THO, Gawler Craton in Australia) are always associated with recycled (Archean) crust. By contrast, juvenile Proterozoic crust is characterized by low heat flux (e.g., all the juvenile belts of the THO, the Proterozoic rocks of the Kola peninsula).

Within each province, there is regional (on a scale on the order of 400 km) variability which must be considered when calculating geotherms. This is illustrated in **Table 4** which shows that the regional variability is high within all provinces. Thus, there is no geotherm characteristic of a single province. To illustrate this point, we have calculated geotherms from selected regions from stable North America. The selection covers the extreme regimes within each age group. The crustal models are described in **Table 5** and the variations in thermal conductivity are described in Appendix 4. Geotherms shown in **Figure 17** illustrate two points: (1) there is no direct relation between the geotherm and the age as the

Table 5 Heat flux crustal heat production used for geotherm calculations

Region	Q_0	A_1	H_1	A_2	H_2	A_3	H_3	Moho depth	T_m
Archean									
E. Abitibi (1)	29	0.4	40					40	325
W. Abitibi (1)	45	1.2	20	0.4	20			40	422
Slave (2)	50	1.7	10	1.2	10	0.4	20	40	428
Proterozoic									
Labrador (3)	22	0.2	40					40	287
THO (Flin Flon Belt)	40	0.3	8	1.2	12	0.25	20	40	434
Wopmay (4)	90	4.8	10	1.0	10	0.4	20	40	705
Grenville (1)	40	0.7	40					40	440
Paleozoic									
Appalachians (1)	58	3.1	8	1.1	10	0.4	22	40	426

References: (1) Mareschal *et al.* (2000); (2) Mareschal *et al.* (2004); (3) Mareschal *et al.* (2000); (4) Lewis *et al.* (2003).

profiles from different age groups overlap; (2) there is also no simple relationship between the surface heat flux and the temperature profiles. For example, there may be no difference in mantle temperature between the Grenville and the Appalachians in spite of the higher surface heat flux in the Appalachians than in the Grenville (58 vs 41 mW m^{-2}). The high heat flux in the Appalachians is mostly accounted for by high heat production (3 μW m^{-3}) at shallow depth resulting in a differentiation index $D_I = 2.5$. In contrast, the Grenville whose crust is made up of stacked slices from all levels appears to be more homogeneous at crustal scale with $D_I = 1$. Thus, the vertical differentiation of the radioelements must be understood in order to estimate Moho and mantle temperatures.

On the scale of the whole North American continent, the average heat production and the crustal differentiation index are positively correlated (Perry *et al.*, 2006). Thus, regions with large heat production (and hence high surface heat flux) are systematically associated with an enriched upper crust. In most cases, this is due to highly radiogenic granites which do not extend very deep, as in the Appalachians province for example. All else being equal, temperatures decrease with increasing differentiation index and increase with increasing heat production. With the correlation between heat production and differentiation index (**Figure 14**), variations of crustal temperatures are much smaller than for a single universal model for the vertical distribution of radioelements. From the standpoint of large-scale geophysical models, the relations between surface heat flux, Moho heat flux, and Moho temperature are nonlinear and cannot be reduced to simple correlations.

6.05.4.5 Variations of Crustal Thickness

Independent evidence for significant horizontal variations of crustal temperatures is provided by the topography of the Moho discontinuity. The characteristic time of relaxation for topography on an interface between two layers with a density difference $\Delta\rho$ is (Chandrasekhar, 1961)

$$\tau \approx \frac{8\pi\mu_{\text{eff}}}{g\,\Delta\rho\,\lambda} \qquad [26]$$

where g is the acceleration of gravity, μ_{eff} an effective viscosity, and λ is the wavelength of the interface topography. The value above yields only an order of magnitude because the relaxation time is modulated by a function depending on the geometry and the boundary conditions (Chandrasekhar, 1961). For representative crustal rheologies, temperature differences of 100–200 K that are predicted imply that the effective viscosity varies by up to three orders of magnitude. Thus, relaxation of tectonic deformation proceeds at different rates depending on the crustal heat production. Higher crustal heat production and heat flow during the Archean might thus explain the observation that the Archean Moho is flat, even in regions that have experienced compression. However, a few areas that were deformed during the Proterozoic have preserved thick crustal roots: the Kapuskasing uplift in the Superior Province, the Lynn Lake area in the THO, and the eastern part of the Grenville Front. Thick crust with the same bulk crustal composition than elsewhere would lead to high temperatures at the Moho and in the underlying mantle, which would allow flow in the lower crust and relaxation of the crustal root. The persistence of

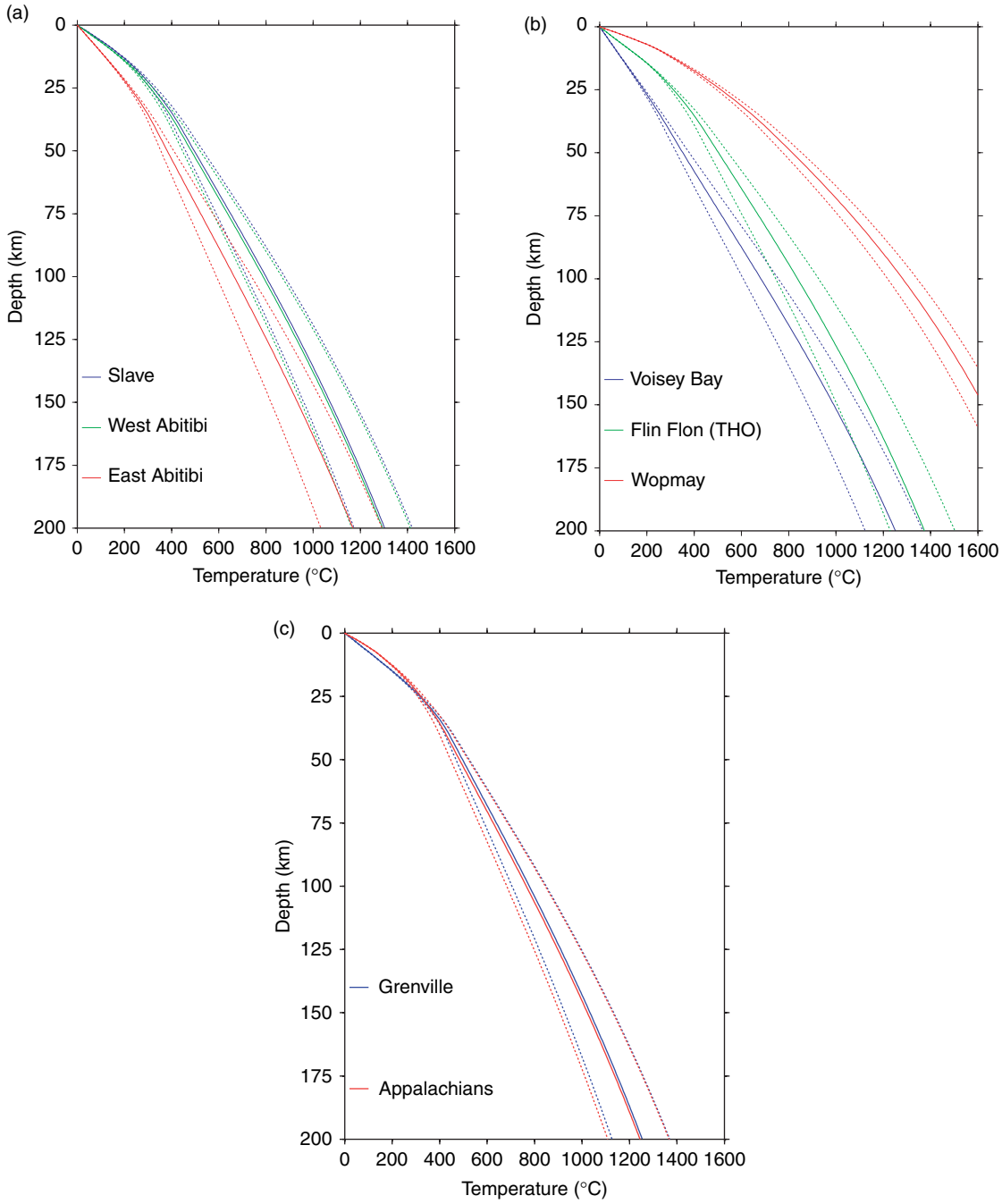

Figure 17 Geotherms for different regions in the Canadian Shield: (a) Eastern Abitibi, western Abitibi, and Slave Province (Archean); (b) Voisey Bay, Flin-Flon Belt, and Wopmay Orogen (Proterozoic), (c) Grenville (Mid-Proterozoic), and Appalachians (Paleozoic). Thick lines are the geotherm calculated for the crustal models in **Table 6**. Thin dotted lines are for the same models with $\pm 2\,\mathrm{mW\,m^{-2}}$ change in Moho heat flow.

crustal roots demonstrates that temperatures have remained low for a very long time (a minimum of 1.8 Gy at both Lynn Lake and Kapuskasing and 1.0 Gy in the Grenville), which can be only explained by anomalously low crustal heat production. Mareschal *et al.* (2005) have indeed noted that heat flux was anomalously low in these two areas of the Canadian Shield.

6.05.4.6 Summary

Continental heat flow is sensitive to the local geology and crustal structure and hence must be used with precaution for studies at the lithospheric scale. In stable continents, high heat flux is always associated with high heat production and an enriched upper crustal layer. Thus, one cannot build geotherms with the same function for the vertical distribution of heat production regardless of the local geological context. Heat flux data alone are not sufficient and must be supplemented by additional information on crustal heat production or mantle heat flux. On a large-scale, three key control variables on lithospheric temperatures are correlated: the average surface heat flux, the average crustal heat production, and the vertical variation of heat production. In contrast, variations in the basal heat flux are small ($\approx \pm 3\,\mathrm{mW\,m^{-2}}$).

Steady-state thermal models are only valid if heat flux is less than about $90\,\mathrm{mW\,m^{-2}}$. Higher values imply melting in the crust or weak lithospheric mantle that can deform easily, suggesting that other heat transport mechanisms are effective. In a thick lithosphere, long-term thermal transients are inevitable.

6.05.5 Continental Lithosphere in Transient Thermal Conditions

6.05.5.1 General Features

In tectonically active regions, advection of heat usually dominates over conduction and temperatures are strongly time dependent. Thermal evolution models depend very much on the choice of the boundary conditions at the base of the lithosphere and cannot be assessed against heat flux data for several reasons. One difficulty comes from the variable quality and density of heat flow data in active regions. In the western US, the numerous heat flux data from the Basin and Range and Rio Grande Rift are very noisy because of hydrological perturbations (Lachenbruch and Sass, 1978), a situation reminiscent of young sea floor. Furthermore, the inclusion in the data set of measurements made for geothermal energy exploration has introduced a strong bias towards excessively high values. Far from thermal steady state, one may not use heat flux data to estimate lithospheric temperatures by downward extrapolation of shallow heat flux measurements.

In a continent that is being deformed, heat flow and temperatures depend on the competing effects of crustal thickness changes, which imply changes of crustal heat production, and deformation, which affect the temperature distribution. Thus, erosion or crustal extension initially cause steeper geotherms and enhanced heat flux. After these transient effects decay, the reduced crustal thickness leads to a lower heat flux than initial. Conversely, crustal thickening causes the geothermal gradient and the heat flux to decrease at first and then to increase due to higher crustal heat production. In many cases, heat flux also records shallow processes such as the cooling of recently emplaced plutons. Because crustal composition is often affected by syn or postorogenic magmatism, there is no general rule to predict the final crustal thickness, composition, and heat-production distribution.

Following the cessation of tectonic and magmatic activity, one must distinguish between two types of transients. Crustal temperatures return to equilibrium with local heat sources in less than 100 My. This is followed by a much slower transient associated with re-equilibration of the lithospheric mantle. For thick lithosphere, such transients may last as long as 500 My (Nyblade and Pollack, 1993; Hamdani *et al.*, 1991; Kaminski and Jaupart, 2000) and result in negative or positive heat flow anomalies. Such slow thermal relaxation has two important features. First, it involves deep thermal anomalies whose lateral variations are efficiently smoothed out by heat conduction and which do not lead to spatial variations of surface heat flux over distances <500 km. Second, it is linked to changes of thermal boundary layer thickness which may be detectable by other methods (Jaupart *et al.*, 1998).

6.05.5.2 Compressional Orogens

Unless the crust has anomalous composition, the total radiogenic heat production increases with crustal thickness. Steady-state conditions have not been reached in young orogens where heat flow is also enhanced by erosion. High heat flux values have been measured in Tibet and parts of the Alps (Jaupart *et al.*, 1985). These values imply high temperatures in the shallow crust. Because these variations are of short wavelengths, they have been attributed to the cooling of shallow plutons. One should note that crustal melting and emplacement of granite intrusions in the upper crust modify the vertical distribution of radioelements. Thus, one should not use the same heat-production model

before and after orogenesis (Sandiford and McLaren, 2002; Mareschal and Jaupart, 2005).

6.05.5.3 Rifts and Zones of Extension

Crustal extension and lithospheric thinning will instantly result in a steeper temperature gradient and an increase in heat flux. Thermal conduction cannot account for the rapid thinning of the lithosphere and mechanical processes such as delamination or diapiric uprise of the asthenosphere are necessary to account for the rapid development of extension zones (Mareschal, 1983). The thermal effects of extension are transient and after return to equilibrium, the heat flux at the surface of thinned crust will reflect the smaller amount of radioactive elements and hence will be lower than before extension. Further changes of crustal heat production may occur due to the injection of basaltic melts, which are depleted in radioelements with respect to average continental crust. This explains, for example, why heat flux is slightly lower in the 1 Gy Keweenawan rift than in the surrounding Superior Province (Perry *et al.*, 2004).

In the Basin and Range Province of the southwestern US (Sass *et al.*, 1994; Morgan, 1983), high heat flux values (110 mW m^{-2}) are consistent with an extension rate of 100% (Lachenbruch and Sass, 1978; Lachenbruch *et al.*, 1994). The high temperatures that are implied must cause thermal expansion of the crust and parts of the mantle and hence should lead to an elevated topography. On the other hand, crustal thinning has the opposite effect. The elevation of the Basin and Range Province cannot be accounted for only by the extension. The calculated thermal expansion in the lithospheric mantle is not sufficient to account for the high elevation. According to Lachenbruch *et al.* (1994), the mantle lithosphere beneath the Basin and Range has been delaminated and not simply stretched.

A striking feature of the zones of extension is that the transition between the region of elevated heat flux and the surrounding is as sharp as the sampling allows to determine. This is observed across the boundaries of the Colorado Plateau and the Basin and Range in North America (Bodell and Chapman, 1982), between the East African Rift and the Tanzanian craton (Nyblade, 1997), or between the Baikal Rift and the Siberian craton (Poort and Klerkx, 2004). Where the sampling is sufficient, heat flux exhibits short-wavelength variations. These variations are probably due to shallow magmatic intrusions, a hypothesis well justified by the numerous volcanic edifices that dot such areas; they also may reflect groundwater movement (Poort and Klerkx, 2004). For studies of lithospheric structure, one must separate between a high background heat flux due to extension and local anomalies reflecting shallow magmatic heat input, which requires measurements at close spacings.

6.05.5.4 Thermal Relaxation of Thick Continental Lithosphere

Once active deformation and magmatism have ceased, the return to thermal equilibrium takes a long time. The thermal relaxation time depends on the thermal structure at the end of activity, the lateral extent of the perturbed region, and the boundary condition at the base of the lithosphere.

6.05.5.4.1 Sedimentary basins

The subsidence of sedimentary basins and passive continental margins provides a good record of the relaxation of thermal perturbations in the lithosphere and is sensitive to lithosphere thickness. Such transients have been recorded in intracratonic basins located away from active plate boundaries and have generated a lot of interest (Haxby *et al.*, 1976; Nunn and Sleep, 1984; Ahern and Mrkvicka, 1984). Subsidence is also affected by tectonic, metamorphic, and eustatic effects. In order to identify these effects, some authors have assumed that the continental lithosphere has a well-defined characteristic cooling time of 60 My (Bond and Kominz, 1991) and that subsidence phases that are significantly longer than this require other causes than thermal effects, such as renewed extension for example. These assumptions are not justified for thick continental lithosphere with long thermal relaxation time.

Theoretical subsidence models that have been developed differ by their initial conditions and their basal boundary conditions (McKenzie, 1978; Hamdani *et al.*, 1991, 1994). Although this has not been sufficiently emphasized, the latter is the important factor determining the duration of thermal subsidence. The duration of the subsidence episode varies by a factor of three between various intracratonic basins of North America. For a fixed temperature at the base of the lithosphere, theory would imply that the continental lithosphere thickness is about 115 km and 270 km beneath the Michigan and Williston basins, respectively (Haxby *et al.*, 1976; Ahern and Mrkvicka, 1984). For two

basins of similar age located on the Precambrian basement of the same continent, such a large difference is surprising. This motivated Hamdani *et al.* (1994) to investigate the influence of thermal boundary conditions at the base of the lithosphere. They showed that subsidence is slower for a fixed flux than for a fixed temperature and attributed the different subsidence behaviors to different thermal processes at the base of the lithosphere. However, these arguments rely on 1-D thermal models which have recently been questioned (Kaminski and Jaupart, 2000). According to Haxby *et al.* (1976), for example, the initial perturbation beneath the Michigan basin has a radius of about 120 km, which is less than the thickness of the North American lithosphere. In this case, the assumption of purely vertical heat transfer is not tenable.

Accounting for horizontal heat transfer, the solution may be cast in the form of a relationship between the width of the thermal perturbation and lithosphere thickness. No solution can be found for lithosphere thicknesses less than 170 km and the observations are best-fitted for a model with fixed heat flux basal boundary condition (Kaminski and Jaupart, 2000).

6.05.5.4.2 Tectonic and magmatic perturbations

The large relaxation time of thick continental lithosphere might lead one to conclude that all thermal perturbations decay slowly and leave a heat flow anomaly for a long time. In some cases where the thermal perturbation is narrow, a large thickness may in a sense be self-defeating as it enhances lateral heat transfer. Thus, thermal relaxation of some tectonic or magmatic perturbations may in fact be more sensitive to width than to thickness.

Gaudemer *et al.* (1988) and Huerta *et al.* (1998) have shown that temperatures in orogenic belts depend on belt width and on local values of heat production and thermal conductivity. One consequence is that (P, T, t) metamorphic paths may record belt width as well as other characteristics. Another striking example is provided by flood basalt provinces where large volumes of magma rose through the lithosphere. For a laterally extensive thermal perturbation, one should detect a relict thermal signal for more than 200 My. There is no heat flow anomaly over the Deccan Traps, India, which erupted about 65 My (Roy and Rao, 2000). The same is true over the Parana basin in Brazil which saw the emplacement of large magma volumes 120 My ago (Hurter and Pollack, 1996). It seems that, in both cases, eruptive fissures are localized in relatively small areas, suggesting that the zone affected by magma ascent may be a few 100 km in width. In this case, thermal perturbations decay rapidly by horizontal heat transport. One consequence is that lithospheric seismic velocity anomalies that are associated with large magmatic events cannot be accounted for by thermal effects and hence reflect compositional variations. In several cases, it seems that the lithosphere has been modified over a large depth interval. For example, a pronounced low-velocity anomaly of narrow width (120 km) extends through the whole mantle part of the lithosphere beneath the south central Saskatchewan kimberlite field in the THO, Canada (Bank *et al.*, 1998). Similar anomalies have been found beneath the Monteregian-White Mountain-New England hotspot track in northeastern America or beneath the Bushveld intrusion in South Africa (Rondenay *et al.*, 2000; James *et al.*, 2001).

6.05.5.5 Long-Term Transients

The large thickness of continental lithosphere implies very large thermal relaxation times with some interesting consequences.

6.05.5.5.1 Archean conditions

The Archean era saw the stabilization of large cratons and the emergence of geological processes that are still active today. In the Archean, crustal metamorphism was biased towards high-temperature–low-pressure conditions in contrast to more recent analogs, indicating that crustal temperatures were higher than today. In apparent contradiction, cratons achieved stability because they had strong lithospheric roots, indicating that temperatures in the lithospheric mantle were not much hotter than today. Proposed mechanisms of formation of lithospheric roots involve either stacking of subducted slabs (Helmstaedt and Schulze, 1989; Abbott, 1991), or melting of mantle over hot spots (Griffin *et al.*, 2003). These mechanisms result in different initial thermal conditions and evolution for the stabilized lithosphere.

In the Archean, heat production in the Earth was double the present, which might suggest higher temperatures in the crust and in the mantle as well as higher heat flux at the base of young continental lithosphere. On average, however, the Archean crust of today is associated with less-heat-producing elements than its modern analogs. When corrected

for age, the total amount of crustal heat production in Archean times was close to that presently observed in Paleozoic provinces. Save for a few anomalous regions with high radioactivity, crustal heat production in the Archean is thus not sufficient to account for crustal temperatures that are higher than those of modern equivalents. The origin of the high-temperature–low-pressure metamorphic conditions must thus be sought in other mechanisms, perhaps widespread magmatic perturbations.

Crustal radioactivity heats the crust in a geologically short time, but a much longer time is required to heat up the lower lithosphere. In Archean times, continental lithosphere was never very old and its thermal structure remained sensitive to initial conditions, that is, conditions which led to the extraction of continental material from the mantle and to the stabilization of thick roots. If the lithospheric mantle is formed by the under-thrusting of subducted slabs beneath the crust, it will initially be colder than in steady state. Mareschal and Jaupart (2005) have estimated the time needed for time-dependent crustal radioactivity to heat up the entire lithosphere. When the half-life of crustal radioactivity is of the same order as the thermal time of the lithosphere, lithospheric temperatures cannot adjust to the time-dependent radiogenic heat production. Following isolation of a continental root from the convecting mantle, the 'radiogenic' temperature component at the base of the lithosphere reaches a maximum after 1–2 Gy, depending on lithospheric thickness (**Figure 18**). The peak temperature is ≈70% of what one would infer from steady-state models with values of heat production at the time of root stabilization. Thus, temperatures in the crust and deep in the continental root are effectively decoupled for a long time. If the root forms with its initial temperature below steady state, the mantle temperature will always be below steady state for the crustal production. Depending on the mechanism of root formation, the lithospheric mantle could well remain sufficiently cold and strong to preserve Archean features (van der Velden *et al.*, 2005).

6.05.5.5.2 Secular cooling in the lithosphere

In thick continental lithosphere, the timescale for diffusive heat transport is comparable to the half-lives of uranium, thorium, and potassium, implying that temperatures are not in equilibrium with the instantaneous rate of radiogenic heat generation. The lithospheric mantle undergoes secular cooling even when thermal conditions at the base of the lithosphere remain steady. The magnitude of transient effects depends on mantle heat production as well

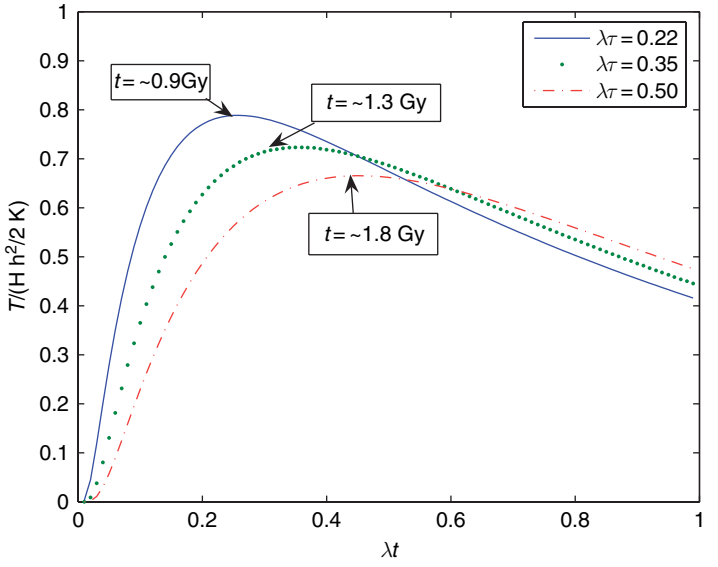

Figure 18 Temperature at the base of the lithospheric root after its stabilization beneath the crust. The temperature is scaled to the maximum temperature increase due to crustal heat production at the time of stabilization. λ is the average decay constant of the radioelements (corresponding to a half-life of about 2.5 Gy). τ is the thermal relaxation time of the root. The chosen values of $\lambda\tau$ correspond to root thickness of 180–250 km.

as on lithosphere thickness. Even large values of heat production do not introduce large transients in a shallow lithosphere. Conversely, even small values of heat production lead to significant transient effects in a thick lithosphere.

In lithosphere that is thicker than 200 km, the geotherm is transient and sensitive to past heat generation. For the same parameters values, and in particular for the same values of present heat production, the deeper part of the temperature profile diverges from a steady-state calculation because of the long time to transport heat to the upper boundary. Depending on the amount of radioelements in the lithospheric mantle, the vertical temperature profile may exhibit significant curvature and may be hotter than a steady-state profile by as much as 150 K (**Figure 19**). For typical values of heat production in the lithospheric mantle, this secular cooling contributes about 3 mW m^{-2} to the total heat flow. Predicted cooling rates for lithospheric material are in the range of 50–150 K Gy^{-1}, close to values reported recently for mantle xenoliths from the Kaapvaal craton, South Africa (Albarède, 2003; Bedini *et al.*, 2004).

One important consequence of such long-term transient behavior stems from the shape of the vertical temperature profile. Applying a steady-state thermal model to xenolith (P, T) data leads to an overestimate of the mantle heat flux and an underestimate of the lithosphere thickness.

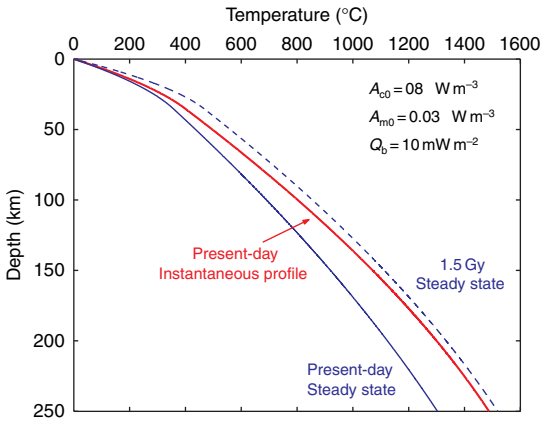

Figure 19 Transient geotherm with decaying heat sources in the lithospheric mantle. Two steady-state calculations corresponding to the same values of heat production today and to values of heat production at 1.5 Gy. Due to the large relaxation time of thick lithosphere, temperatures are not in equilibrium with radioactive heat sources.

6.05.6 Other Geophysical Constraints on the Thermal Regime of the Continental Lithosphere

6.05.6.1 Constraints from Seismology

The 3-D seismic velocity structure of the upper mantle determined by seismic tomography has shown strong correlation with the geology. In particular, the presence of lithospheric roots beneath cratons is associated with higher seismic velocity and lower temperature than outside. Horizontal differences in seismic velocities can be interpreted in terms of compositional and thermal differences. Within the continents, seismic velocities are higher within cratons than outside. There are also smaller-scale differences that cannot be explained in terms of temperature only (Poupinet *et al.*, 2003).

Heat flux data and thermodynamic constraints can be used to narrow down the range of mantle temperatures consistent with seismic tomography models. Shapiro and Ritzwoller (2004) inverted surface-wave data to obtain vertical profiles of S-wave velocity through both continents and oceans. For a given compositional model, these data can be converted to temperature. In a given area, the solution domain allows for nonmonotonic variations of temperature with depth, that is, with zones where temperature decreases with depth, which are not physically realistic. Applying the constraint that temperature must always increase with depth leads to a narrower solution domain. The range can be further narrowed down with constraints from heat flux by eliminating solutions outside the range of Moho temperatures allowed by thermal models. One striking result is that this procedure gets rid of the nonphysical solutions with negative vertical temperature gradients (**Figure 20**).

6.05.6.2 Seismicity, Elastic Thickness, and Thermal Regime of the Lithosphere

In the oceans, both the effective elastic thickness (T_e) and the maximum depth of earthquakes increase with the age of the oceanic lithosphere (Watts, 2001; Seno and Yamanaka, 1996). The dependence of T_e on the age of the oceanic lithosphere (at the time of loading) was examined in many studies (Watts, 2001; Lago and Cazenave, 1981; Calmant *et al.*, 1990) that show that, with few exceptions, oceanic T_e is given approximately by the depth to the 450°C isotherm of the cooling plate model. The thickness of the

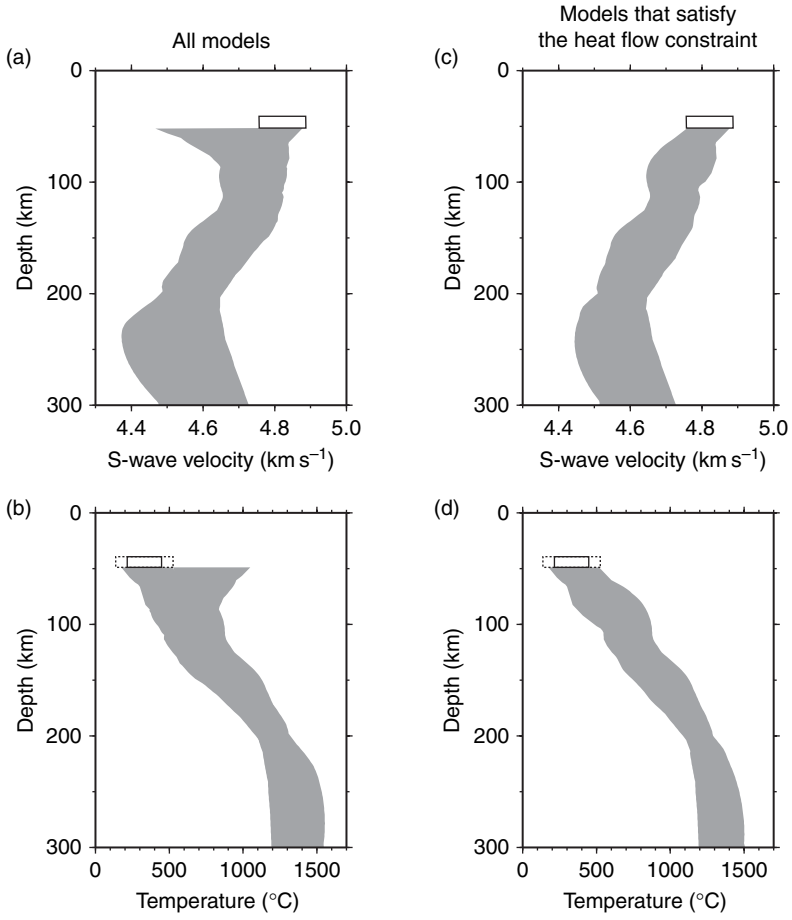

Figure 20 Top: Vertical profiles of S-wave velocity through the Canadian Shield obtained by diffraction tomography. From Shapiro and Ritzwoller (2004) Bottom: Vertical temperature profiles deduced from the velocity data. The left panel shows the whole solution domain, which includes nonphysical temperature profiles such that temperature decreases with depth at shallow levels. The right panel shows the solutions that are consistent with bounds of the Moho temperature deduced from heat flow studies. All the nonrealistic temperature profiles have been eliminated.

seismogenic layer has been determined for intraplate settings or seaward of deep trenches (Wiens and Stein, 1984; Seno and Yamanaka, 1996). This thickness follows closely the T_e estimates suggesting that in the ocean, the brittle-to-ductile transition occurs at <600°C.

The effective elastic thickness of the lithosphere is related to the yield strength envelope which is useful to understand how the temperature profile affects the strength of the lithosphere. The depth where the strength begins to decrease corresponds to the transition from brittle to ductile. In the oceans, this depth is strongly controlled by temperature, that is, by the age of the plate (McKenzie *et al.*, 2005).

In the continents, the strength profile is complicated by the rheological stratification in the lithosphere. A relationship between age, thermal regime, and strength of the continental lithosphere was suggested by Karner *et al.* (1983). This clearly holds for the very young lithosphere and explains differences between the elastic thickness in the Basin and Range and stable North America (Lowry and Smith, 1995). The seismogenic zone is usually shallow (<30 km) beneath the continents suggesting a ductile lithosphere (Maggi *et al.*, 2000). This is inconsistent with the large values of T_e (>80 km) observed beneath cratons that require a cold lithosphere. The temperature differences inferred from thermal models are consistent with the very long wavelength variations in elastic thickness. Small-scale variations in T_e are much more difficult to account for by the thermal regime.

6.05.6.3 Depth to the Curie Isotherms

The main sources of magnetic anomalies are present in the crust and not in the mantle. The Curie isotherm for magnetite, ≈580°C, will normally be located in the upper mantle beneath continents and oceans. However, high surface heat flux and elevated temperatures in the lower crust will cause a shallow Curie isotherm with thinning of the magnetic crust and a local source of magnetic anomaly. Satellite magnetic data are useful to estimate the depth to the Curie isotherm (Hamoudi *et al.*, 1998). The high-quality magnetic data obtained by recent satellite missions have sufficient resolution to be useful for lithospheric studies (Maus *et al.*, 2006). Satellite magnetic data have been used to confirm the elevated lower crustal temperatures beneath the Basin and Range (Mayhew, 1982) or to delineate the edge of the North American craton (Purucker *et al.*, 2002).

6.05.6.4 Thermal Isostasy

In the oceans, long-wavelength bathymetric variations are caused by density variations in the lithosphere. The depth of sea floor below sea level is directly related to the average lithospheric density and temperature. Note that the oceanic geotherm is not in steady state. Crough and Thompson (1977) have applied similar concepts to the continental lithosphere. In the continents, density variations are due more to changing crustal thickness (and composition) than to differences in temperature. Low mantle temperature beneath the cratons should increase the density of the mantle and keep the elevation much lower than the observed mean elevation. This observation led Jordan (1981) to propose that the cratonic mantle is made up of refractory residual mantle with lower density than the off-cratonic mantle. This compositional effect balances the thermal effect to give to the cratons their present elevation.

The component of the topography of the continents due to thermal isostasy is usually small, except in regions of extension. In the Basin and Range, where the typical crustal thickness is 30 km, the average elevation of 1750 m requires the upper-mantle density to be anomalously low. Differences in temperature can account only for part of the elevation, and low-density magma intrusions are thought to also contribute to the buoyancy of the mantle (Lachenbruch and Morgan, 1990). The high heat flow in the Canadian Cordillera suggests that thermal isostasy contributes to part of the elevation (Lewis *et al.*, 2003). The buoyancy of the mantle beneath the Colorado Plateau is likely to be in part thermal, although the heat flow is not high in the Plateau, possibly because not enough time has elapsed to allow the effect of higher mantle temperature to be conducted to the surface (Bodell and Chapman, 1982).

6.05.7 Conclusions

Ironically, Kelvin's calculation applies to large parts of the Earth surface and does lead to an accurate prediction of age. The age, however, is not that of the planet but that of its oceanic plates. The failure of this simple model to account for heat flux and bathymetry of old sea floor provides very useful information on the heat transport mechanisms that are active in the mantle and helps addressing the more complex problem of continents. The mechanism which brings heat to the base of the oceanic lithosphere is probably also active beneath the continental lithosphere and explains why continents tend to thermal steady state.

Lithosphere thickness is in many ways an ill-defined variable. Not only does its value vary from one geophysical method to the next, but from the thermal perspective it may also change depending on the basal boundary condition. Furthermore, it may be different for steady-state and transient thermal models. Such complexities are not merely a problem of vocabulary and reflect important features of heat transport in the upper boundary layer of mantle convection.

For lithospheric studies, one should regard heat flow data as affected by large geological noise. The sources of this noise are hydrothermal circulation in the oceans, and crustal radiogenic heat production in the continents. Unfortunately, this noise is locally controlled (i.e., local topography and sediment thickness for oceans, geological evolution and crustal structure for continents). Thus, one may not propose generic lithosphere models valid for continents or oceans of given age without carefully accounting for the local environment. One may not determine lithosphere structure without additional constraints and without a heat transport model. Heat flow data, however, do provide strong constraints on heat transport mechanisms.

Appendix 1: Measurement Techniques

Heat flux is never directly measured but its vertical component is obtained by the Fourier's law

$$Q = k\frac{\partial T}{\partial z} \quad [27]$$

Continental or oceanic heat flux measurements thus require the determination of the vertical temperature gradient and thermal conductivity (Beck, 1988; Jessop, 1990).

Conventional Land Heat Flow Measurements

On land, conventional heat flow measurements are obtained by measuring temperature in drill-holes (usually holes of opportunity, mostly mining exploration). Continuous core samples are routinely kept in mining exploration, and conductivity can be measured on samples from the hole. The divided bar method provides the most robust measurement of the bulk rock conductivity because it involves relatively large samples and is insensitive to small-scale variations in lithology, but it is time consuming and only a limited number of samples can be processed. Continuous measurement of conductivity on the entire core can be made with an optical scanning device (Popov *et al.*, 1999). The heat flow is commonly obtained as the slope of the best-fitting line to the 'Bullard plot' of temperature versus thermal resistivity $R(z)$:

$$R(z) = \int_0^z \frac{\mathrm{d}z'}{k(z')} \quad [28]$$

Alternatively, heat flux can be obtained from Fourier's law over depth intervals where the conductivity is constant. Both methods give comparable results even when the fit is poor or when heat flow varies between depth intervals. Because the temperature field in the upper 200 m is often perturbed by surface effects, including the effect of recent climate change, reliable heat flow measurements require deep boreholes (at least 300 m).

Bottom Hole Temperature (BHT) Data

Temperature measurements are also routinely available from oil exploration wells, either as BHT or drillstem tests, with a precision never better than 5–10 K after corrections. In these deep wells, the gradient can thus be estimated with a precision of 10–15%. The other difficulty of these measurements is the lack of core samples for thermal conductivity, which has to be estimated from the lithology or from other physical properties (density, porosity, etc.) that are routinely logged. Although, less precise than conventional methods, these data have provided most of the estimates of heat flux in sedimentary basins and on many continental margins.

Appendix 2: Corrections

Heat flux determinations assume that heat is transported vertically in steady state, and thus require no lateral variations in surface boundary conditions or physical properties. Changes in vegetation, the proximity to a lake, topography can distort the temperature field and affect the heat flow estimate (Jeffreys, 1938). Rapid erosion (or sedimentation) also affects the temperature field (Benfield, 1949). These effects are largest near the surface and the error on the heat flow is small in sufficiently deep boreholes. The effect of a lake or change in vegetation cannot be estimated without extensive data coverage in the horizontal direction but topographic effect can be accounted for and corrections can be made. If the erosion rate is known, a correction can also be applied (Carslaw and Jaeger, 1959, p. 388).

Appendix 3: Climatic Effects

Temperatures near the Earth surface keep a memory of the past surface boundary conditions. This was understood by Kelvin who tried to use this memory to determine the age of the Earth (Thomson, 1864). For a periodic variations of the surface temperature, the temperature wave is attenuated exponentially as it propagates downward with a skin depth $\delta = \sqrt{\kappa T/\pi}$ (Carslaw and Jaeger, 1959, page 66), where T is the period and κ the thermal diffusivity. The daily and annual temperature cycles are damped over less than 0.5 or 10 m. They do not affect temperature at the depth of land heat flux measurements. Long-term variations in surface temperature could potentially significantly affect the temperature gradient. Birch (1948) had already pointed out that, following the last glacial episode that ended *c.* 10 000 years BP, surface temperature warming could affect the temperature gradient down to 2000 m and, if not accounted for, lead to underestimating the heat flow. If the time-varying surface

boundary condition was known, it would be easy to account for it and make a correction. For the part of Canada covered by the Laurentide ice sheet, Jessop (1971) proposed a correction for a detailed climate history of the past 400 000 years with temperature equal to present during the interglacials and to −1°C during the glacial episodes. Because the present temperature of the ground surface in Canada is quite low, the correction is usually small (<10% the heat flux). Measurements in deep boreholes in Canada have indeed shown that heat flow does not increase much at depth and that the effect of last glaciation is small (Sass *et al.*, 1971; Rolandone *et al.*, 2003). These measurements also show that the thermal boundary condition at the base of the glacier might have been quite variable (possibly because it depends on the heat flow). Without detailed information on this past boundary condition, identical corrections have been applied to all the data from Canada. Similar corrections have been applied to the data from Siberia.

During the past 200 years, there has been a general warming trend following the 'Little Ice Ages' with an acceleration since 1960. This recent warming affects temperature profiles down to 200 m. In regions where heat flux is low and the warming has been particularly strong, the temperature gradients are inverted down to 50–80 m. Borehole temperature profiles have been inverted to determine the surface temperature of the past centuries (Cermak, 1971; Lachenbruch and Marshall, 1986; Lewis, 1992). For measuring heat flux, it is now clear that reliable estimates require relatively deep boreholes (>300 m) to filter out the effect of recent warming and measure a stable temperature gradient over >100 m.

Appendix 4: Physical Properties

The calculation of the geotherm requires thermal conductivity to be known. Thermal conductivity depends on composition: it increases with the quartz content (Clauser and Huenges, 1995, and references therein). **Table 6** gives values of thermal conductivity for some important rocks and minerals. The lattice conductivity decreases with temperature. Over the range of crustal temperatures, the thermal conductivity can vary by as much as 50%. Durham *et al.* (1987) have measured the thermal conductivity variations for samples of different crustal rocks and proposed the following law for the thermal conductivity in the crust:

Table 6 Thermal conductivity of some rocks at room temperature

Rock type	Mean ($W\,m^{-1}\,K^{-1}$)	Min–max ($W\,m^{-1}\,K^{-1}$)	References
Basalt	2.0	1.8–2.5	Clark (1966)
Gabbro	2.2	1.8–2.5	Clark (1966)
Gneiss	3.6	2.0–5.0[a]	Clauser and Huenges (1995)
Granite	3.2	2.8–3.6	Clark (1966)
Granulite facies rocks	—	3.01–3.48	Joeleht and Kukkonen (1998)
Peridotite	2.8	2.3–3.4	Clark (1966)

[a]Thermal conductivity of gneiss in direction perpendicular to foliation is 0.6 that parallel to foliation.

$$K = 2.26 - \frac{618.241}{T} + K_0\left(\frac{255.576}{T} - 0.30247\right) \quad [29]$$

where K is thermal conductivity (in $W\,m^{-1}\,K^{-1}$), T is the absolute temperature, and K_0 is the conductivity at the surface (for $T = 273$ K). Clauser and Huenges (1995) propose similar equations to determine the lattice conductivity. The temperature dependence of conductivity cannot be neglected. When calculated with temperature-dependent conductivity, Moho temperatures are ≈150 K higher than for constant conductivity.

At temperature higher than 1000 K, the radiative component to the thermal conductivity must be included. For mantle rocks, the radiative component can be calculated as (Schärmeli, 1979)

$$K_r = 0.37 \times 10^{-9} T^3 \quad [30]$$

The specific heat of crustal rocks is ≈1000 $J\,kg^{-1}\,K^{-1}$. The thermal diffusivity is ≈10^{-6} $m^2\,s^{-1}$, that is, 31.5 $m^2\,y^{-1}$.

References

Abbott D (1991) The case for accretion of the tectosphere by buoyant subduction. *Geophysical Research Letters* 18: 585–588.

Ahern J and Mrkvicka S (1984) A mechanical and thermal model for the evolution of the Williston basin. *Tectonics* 3: 79–102.

Albarède F (2003) The thermal history of leaky chronometers above their closure temperature. *Geophysical Research Letters* 30, doi:10.1029/2002GL016484.

Artemieva IM and Mooney WD (2001) Thermal thickness and evolution of Precambrian lithosphere: A global study. *Journal of Geophysical Research* 106: 16387–16414.

Ashwal LD, Morgan P, Kelley SA, and Percival J (1987) Heat production in an Archean crustal profile and implications for heat flow and mobilization of heat producing elements. *Earth and Planetary Science Letters* 85: 439–450.

Ballard S, Pollack HN, and Skinner NJ (1987) Terrestrial heat flow in Botswana and Namibia. *Journal of Geophysical Research* 92: 6291–6300.

Bank C-G, Bostock MG, Ellis RM, Hajnal Z, and VanDecar JC (1998) Lithospheric mantle structure beneath the Trans-Hudson Orogen and the origin of diamondiferous kimberlites. *Journal of Geophysical Research* 103: 10103–10114.

Bea F and Montero P (1999) Behaviour of accessory phases and redistribution of Zr, REE, Y, th, and U during metamorphism and partial melting of metapelites in the lower crust: An example from the Kinzigite formation of Ivrea–Verbano, northwestern Italy. *Geochimica et Cosmochimica Acta* 63: 1133–1153.

Beck AE (1988) Methods for determining thermal conductivity and thermal diffusivity. In: Haenel R, Rybach L, and Stegena L (eds.) *Handbook of Terrestrial Heat Flow Density Determination*, pp. 87–124. Dordrecht: Kluwer.

Becker K and Davis E (2004) *In situ* determinations of the permeability of the igneous oceanic crust. In: Davis E and Elderfield H (eds.) *Hydrogeology of the Oceanic Lithosphere*, pp. 189–224. Cambridge: Cambridge University Press.

Bedini R-M, Blichert-Toft J, Boyet M, and Albarède F (2004) Isotopic constraints on the cooling of the continental lithosphere. *Earth and Planetary Science Letters* 223: 99–111.

Benfield AE (1949) The effect of uplift and denudation on underground temperatures. *Journal of Applied Physiology* 20: 66–70.

Bingen B, Demaiffe D, and Hertogen J (1996) Redistribution of rare earth elements, thorium, and uranium over accessory minerals in the course of amphibolite to granulite facies metamorphism: The role of apatite and monazite in orthogneisses from southwestern Norway. *Geochimica et Cosmochimica Acta* 60: 1341–1354.

Birch F (1948) The effects of Pleistocene climatic variations upon geothermal gradients. *American Journal of Science* 246: 729–760.

Birch F (1965) Speculations on the earth thermal history. *Geological Society of America Bulletin* 76: 133–154.

Birch F, Roy RF, and Decker ER (1968) Heat flow and thermal history in New England and New York. In: An-Zen E (ed.) *Studies of Appalachian Geology*, pp. 437–451. New York: Wiley-Interscience.

Blackwell D and Richards M (2004) *Geothermal Map of North America*. Tulsa: American Association of Petroleum Geologists.

Bodell JM and Chapman DS (1982) Heat flow in the north central Colorado plateau. *Journal of Geophysical Research* 87: 2869–2884.

Bond G and Kominz M (1991) Disentangling middle Paleozoic sea level and tectonic events in cratonic margins and cratonic basins of North America. *Journal of Geophysical Research* 94: 6619–6639.

Bonneville A, Von Herzen RP, and Lucazeau F (1997) Heat flow over Reunion hot spot track: Additional evidence for thermal rejuvenation of oceanic lithosphere. *Journal of Geophysical Research* 102: 22731–22748.

Brady RJ, Ducea MN, Kidder SB, and Saleeby JB (2006) The distribution of radiogenic heat production as a function of depth in the Sierra Nevada batholith, California. *Lithos* 86: 229–244.

Bullard EC (1939) Heat flow in South Africa. *Proceeding of the Royal Society of London Series A* 173: 474–502.

Bullard EC (1954) The flow of heat through the floor of the Atlantic ocean. *Proceeding of the Royal Society of London Series A* 222: 408–422.

Calmant S, Francheteau J, and Cazenave A (1990) Elastic layer thickening with age of the oceanic lithosphere. *Geophysical Journal International* 100: 59–67.

Carlson RL and Johnson HP (1994) On modeling the thermal evolution of the oceanic upper mantle: An assessment of the cooling plate model. *Journal of Geophysical Research* 99: 3201–3214.

Carlson RW, Pearson DG, and James DE (2005) Physical, chemical, and chronological characteristics of continental mantle. *Reviews of Geophysics* 43: RG1001 (doi:10.1029/2004RG000156).

Carslaw HS and Jaeger JC (1959) *Conduction of Heat in Solids,* 2nd edn. Oxford: Clarendon Press.

Cermak V (1971) Underground temperature and inferred climatic temperature of the past millenium. *Palaeogeography Palaeoclimatology Palaeoecology* 98: 167–182.

Chandrasekhar S (1961) *Hydrodynamic and Hydromagnetic Stability*. Oxford: Oxford University Press.

Clark SP (1966) Thermal conductivity. In: Clark SP (ed.) *Handbook of Physical Constants*, pp. 459–482. Boulder: GSA.

Clauser C and Huenges E (1995) Thermal conductivity of rocks and minerals. In: Ahrens TJ (ed.) *A Handbook of Physical Constants: Rock Physics and Phase Relations*, pp. 105–126. Washington: AGU.

Courtney R and White R (1986) Anomalous heat flow and geoid across the Cape Verde Rise: Evidence of dynamic support from a thermal plume in the mantle. *Geophysics Journal of the Royal Astronomical Society* 87: 815–868.

Crough ST (1983) Hotspot swells. *Annual Review of Earth and Planetary Sciences* 11: 165–193.

Crough ST and Thompson GA (1977) Thermal model of continental lithosphere. *Journal of Geophysical Research* 81: 4857–4862.

Cull JP (1991) Heat flow and regional geophysics in Australia. In: Cermak V and Rybach L (eds.) *Terrestrial Heat Flow and the Lithosphere Structure*, pp. 486–500. Berlin: Springer-Verlag.

Davaille A and Jaupart C (1994) Onset of thermal convection in fluids with temperature-dependent viscosity: Application to the oceanic mantle. *Journal of Geophysical Research* 99: 19853–19866.

Davies GF (1988) Ocean bathymetry and mantle convection, 1. Large-scale flow and hotspots. *Journal of Geophysical Research* 93: 10467–10480.

Davis EE and Elderfield H (2004) *Hydrogeology of the Oceanic Lithosphere*. Cambridge: Cambridge University Press.

Davis EE and Lister CRB (1974) Fundamentals of ridge crest topography. *Earth and Planetary Science Letters* 21: 405–413.

Davis EE, Chapman DS, Wang K, *et al.* (1999) Regional heat flow variations across the sedimented Juan de Fuca ridge eastern flank: Constraints on lithospheric cooling and lateral hydrothermal heat transport. *Journal of Geophysical Research* 104: 17675–17688.

Decker ER, Baker KR, Bucher GJ, and Heasler HP (1980) Preliminary heat flow and radioactivity studies in Wyoming. *Journal of Geophysical Research* 85: 311–321.

Doin M-P and Fleitout L (1996) Thermal evolution of the oceanic lithosphere: An alternative view. *Earth and Planetary Science Letters* 142: 121–136.

Doin M-P, Fleitout L, and McKenzie D (1996) Geoid anomalies and the structure of continental and oceanic lithospheres. *Journal of Geophysical Research* 101: 16119–16136.

Dumoulin C, Doin M, and Fleitout L (2001) Numerical simulations of the cooling of an oceanic lithosphere above a

convective mantle. *Physics of the Earth and Planetary Interiors* 125: 45–64.
Durham WB, Mirkovich VV, and Heard HC (1987) Thermal diffusivity of igneous rocks at elevated pressure and temperature. *Journal of Geophysical Research* 92: 11615–11634.
Fountain DM, Salisbury MH, and Furlong KP (1987) Heat production and thermal conductivity of rocks from the Pikwitonei–Sachigo continental cross-section, central Manitoba: Implications for the thermal structure of Archean crust. *Canadian Journal of Earth Sciences* 24: 1583–1594.
Fourier JBJ (1820) Extrait d'un mémoire sur le refroidissement du globe terrestre. *Bulletin des Sciences de la Societe Philomathique de Paris*.
Gass IG, Thorpe RS, Pollack HN, and Chapman DS (1978) Geological and geophysical parameters for mid-plate volcanism. *Philosophical Transactions of the Royal Society of London Series A* 301: 581–597.
Gaudemer Y, Jaupart C, and Tapponier P (1988) Thermal control on post-orogenic extension in collision belts. *Earth and Planetary Science Letters* 89: 48–62.
Griffin WL, O'Reilly SY, Abe N, *et al.* (2003) The origin and evolution of Archean lithospheric mantle. *Precambrian Research* 127: 19–41.
Guillou L, Mareschal JC, Jaupart C, Gariépy C, Bienfait G, and Lapointe R (1994) Heat flow and gravity structure of the Abitibi belt, Superior Province, Canada. *Earth and Planetary Science Letters* 122: 447–460.
Gung Y, Panning M, and Romanowiz B (2003) Global anisotropy and the thickness of the continents. *Nature* 422: 707–710.
Hamdani Y, Mareschal J-C, and Arkani-Hamed J (1991) Phase change and thermal subsidence basins. *Geophysical Journal International* 106: 657–665.
Hamdani Y, Mareschal J-C, and Arkani-Hamed J (1994) Phase change and thermal subsidence of the Williston basin. *Geophysical Journal International* 116: 585–597.
Hamoudi M, Cohen Y, and Achache J (1998) Can the thermal thickness of the continental lithosphere be estimated from Magsat data. *Tectonophysics* 284: 19–29.
Harris RN and Chapman DS (2004) Deep-seated oceanic heat flow heat deficits, and hydrothermal circulation. In: Dovis E and Elderfield H (eds.) *Hydrogeology of the Oceanic Lithosphere*, pp. 311–336. Cambridge: Cambridge University Press.
Harris RN, Garven G, Georgen J, McNutt MK, Christiansen L, and Von Herzen RP (2000) Submarine hydrogeology of the Hawaiian archipelagic apron 2. Numerical simulations of coupled heat transport and fluid flow. *Journal Geophysical Research* 105: 21353–21370.
Haxby W, Turcotte D, and Bird J (1976) Thermal and mechanical evolution of the Michigan basin. *Tectonophysics* 36: 57–75.
Haxby WF and Turcotte DL (1978) On isostatic geoid anomalies. *Journal of Geophysical Research* 83: 5473–5478.
Heestand RL and Crough ST (1981) The effect of hot spots on the oceanic age–depth relation. *Journal of Geophysical Research* 86: 6107–6114.
Helmstaedt HH and Schulze DJ (1989) Southern African kimberlites and their mantle sample: Implications for Archean tectonics and lithosphere evolution. In: Ross J (ed.) *Geological Society of Australia Special Publication: Kimberlites and Related Rocks: Volume 1. Their Composition, Occurrence, Origin, and Emplacement*, vol. 14, pp. 358–368. Sydney: Geological Society of Australia.
Hirth G and Kohlstedt DL (1996) Water in the oceanic upper mantle: Implications for rheology, melt extraction and the evolution of the lithosphere. *Earth and Planetary Science Letters* 144: 93–108.
Hirth G, Evans R, and Chave A (2000) Comparison of continental and oceanic mantle electrical conductivity: Is the Archean lithosphere dry? *Geochemistry Geophysics Geosystems* 1: 2000GC000,048.
Holmes A (1915) Radioactivity and the earth's thermal history: Part 1. The concentration of radioactive elements in the earth's crust. *Geological Magazine* 2: 60–71.
Huang J and Zhong S (2005) Sublithospheric small-scale convection and its implications for the residual topography at old ocean basins and the plate model. *Journal of Geophysical Research* 110: B05404 (doi:10.1029/2004JB003153).
Huerta AD, Royden LH, and Hodges KV (1998) The thermal structure of collisional orogens as a response to accretion, erosion, and radiogenic heating. *Journal of Geophysical Research* 103: 15287–15302.
Humler E, Langmuir C, and Daux V (1999) Depth versus age: New perspectives from the chemical compositions of ancient crust. *Earth and Planetary Science Letters* 173: 7–23.
Hurter SJ and Pollack HN (1996) Terrestrial heat flow in the Paraná Basin, southern Brazil. *Journal of Geophysical Research* 101: 8659–8672.
James DE, Fouch MJ, VanDecar JC, and van der Lee S (2001) Tectospheric structure beneath southern Africa. *Geophysical Research Letters* 28: 2485–2488.
Jaupart C (1983a) Horizontal heat transfer due to radioactivity contrasts: Causes and consequences of the linear heat flow–heat production relationship. *Geophysical Journal of the Royal Astronomical Society* 75: 411–435.
Jaupart C (1983b) The effects of alteration and the interpretation of heat flow and radioactivity data – a reply to R. U. M. Rao. *Earth and Planetary Science Letters* 62: 430–438.
Jaupart C and Mareschal JC (1999) The thermal structure and thickness of continental roots. *Lithos* 48: 93–114.
Jaupart C and Mareschal JC (2003) Constraints on crustal heat production from heat flow data. In: Rudnick RL (ed.) *Treatise on Geochemistry, The Crust*, vol. 3, pp. 65–84. New York: Permagon.
Jaupart C, Francheteau J, and Shen X-J (1985) On the thermal structure of the southern Tibetan crust. *Geophysics Journal of the Royal Astronomical Society* 81: 131–155.
Jaupart C, Mareschal JC, Guillou-Frottier L, and Davaille A (1998) Heat flow and thickness of the lithosphere in the Canadian Shield. *Journal of Geophysical Research* 103: 15269–15286.
Jeffreys H (1938) The disturbance of the temperature gradient in the Earth's crust by inequalities of height. *Monthly Notices of the Royal Astronomical Society. Geophysical Supplement* 4: 309–312.
Jessop AM (1971) The distribution of glacial perturbation of heat flow in Canada. *Canadian Journal of Earth Sciences* 8: 162–166.
Jessop AM (1990) *Thermal Geophysics*. Amsterdam: Elsevier.
Joeleht TH and Kukkonen IT (1998) Thermal properties of granulite facies rocks in the Precambrian basement of Finland and Estonia. *Tectonophysics* 291: 195–203.
Johnson HP and Carlson RL (1992) Variation of sea floor depth with age: A test of models based on drilling results. *Geophysical Research Letters* 19: 1971–1974.
Jones MQW (1987) Heat flow and heat production in the Namaqua mobile belt, South Africa. *Journal of Geophysical Research* 92: 6273–6289.
Jones MQW (1988) Heat flow in the Witwatersrand Basin and environs and its significance for the South African Shield geotherm and lithosphere thickness. *Journal of Geophysical Research* 93: 3243–3260.
Jordan TH (1975) The continental tectosphere. *Reviews of Geophysics and Space Physics* 13: 1–12.

Jordan TH (1981) Continents as a chemical boundary layer. *Royal Society of London Philosophical Transactions Series A* 301: 359–373.

Jurine D, Jaupart C, Brandeis G, and Tackley PJ (2005) Penetration of mantle plumes through depleted lithosphere. *Journal of Geophysical Research* 110: B10104 (doi:10.1029/2005JB003751).

Kaminski E and Jaupart C (2000) Lithospheric structure beneath the Phanerozoic intracratonic basins of North America. *Earth and Planetary Science Letters* 178: 139–149.

Karner GD, Steckler MS, and Thorne J (1983) Long-term mechanical properties of the continental lithosphere. *Nature* 304: 250–253.

Ketcham RA (1996) Distribution of heat-producing elements in the upper and middle crust of southern and west central Arizona: Evidence from the core complexes. *Journal of Geophysical Research* 101: 13,611–13,632.

Kinzler RJ and Grove TL (1992) Primary magmas of mid-ocean ridge basalts 2. Applications. *Journal of Geophysical Research* 97: 6907–6926.

Klein EM and Langmuir CH (1987) Global correlations of ocean ridge basalt chemistry with axial depth and crustal thickness. *Journal of Geophysical Research* 92: 8089–8115.

Kremenentsky AA, Milanovsky SY, and Ovchinnikov LN (1989) A heat generation model for the continental crust based on deep drilling in the Baltic shield. *Tectonophysics* 159: 231–246.

Kukkonen IT, Golovanova YV, Druzhinin VS, Kosarev AM, and Schapov VA (1997) Low geothermal heat flow of the Urals fold belt: Implication of low heat production, fluid circulation or paleoclimate. *Tectonophysics* 276: 63–85.

Kutas RI (1984) Heat flow, radiogenic heat production, and crustal thickness in southwest USSR. *Tectonophysics* 103: 167–174.

Lachenbruch AH (1970) Crustal temperature and heat production: Implications of the linear heat flow heat production relationship. *Journal of Geophysical Research* 73: 3292–3300.

Lachenbruch AH and Marshall BV (1986) Changing climate: Geothermal evidence from permafrost in Alaska. *Science* 234: 689–696.

Lachenbruch AH and Morgan P (1990) Continental extension, magmatism and elevation; formal relations and rules of thumb. *Tectonophysics* 174: 39–62.

Lachenbruch AH and Sass JH (1978) Models of an extending lithosphere and heat flow in the Basin and Range Province. *Memoirs of the Geological Society of America* 152: 209–258.

Lachenbruch AH, Sass JH, and Morgan P (1994) Thermal regime of the southern Basin and Range Province: 2. Implications of heat flow for regional extension and metamorphic core complexes. *Journal of Geophysical Research* 99: 22121–22133.

Lago B and Cazenave A (1981) State of stress of the oceanic lithosphere in response to loading. *Geophysical Journal of the Royal Astronominal Society* 64: 785–799.

Lago B, Cazenave A, and Marty J-C (1990) Regional variations in subsidence rate of lithospheric plates: Implication for thermal cooling models. *Physics of the Earth and Planetary Interiors* 61: 253–259.

Lee MK, Brown GC, Webb PC, Wheildon J, and Rollin KE (1987) Heat flow, heat production and thermo-tectonic setting in mainland UK. *Journal of the Geological Society* 144: 35–42.

Lewis TJ (1992) (Ed.) Climatic change inferred from underground temperatures. *Palaeogeography Palaeoclimatology Palaeoecology* 98: 78–282.

Lewis TJ, Hyndman RD, and Fluck P (2003) Heat flow, heat generation and crustal temperatures in the northern Canadian Cordillera: Thermal control on tectonics. *Journal of Geophysical Research* 108: 2316.

Li X, Kind R, Yuan X, Wölbern I, and Hanka W (2004) Rejuvenation of the lithosphere by the Hawaiian plume. *Nature* 427: 827–829.

Lister CRB (1977) Estimators for heat flow and deep rock properties based on boundary layer theory. *Tectonophysics* 41: 157–171.

Lister CRB, Sclater JG, Nagihara S, Davis EE, and Villinger H (1990) Heat flow maintained in ocean basins of great age – Investigations in the north-equatorial West Pacific. *Geophysical Journal International* 102: 603–630.

Lowry AR and Smith BB (1995) Strength and rheology of the western US Cordillera. *Journal of Geophysical Research* 100: 17947–17963.

Maggi A, Jackson JA, McKenzie DP, and Preistley K (2000) Earthquake focal depths, effective elastic thickness, and the strength of the continental lithosphere. *Geology* 28: 495–498.

Mareschal JC (1983) Mechanisms of uplift preceding rifting. *Tectonophysics* 94: 51–66.

Mareschal JC and Jaupart C (2004) Variations of surface heat flow and lithospheric thermal structure beneath the North American craton. *Earth and Planetary Science Letters* 223: 65–77.

Mareschal JC and Jaupart C (2005) Archean thermal regime and stabilization of the cratons. In: Benn K, Condie K, and Mareschal JC (eds.) *Archean Geodynamic Processes*, pp. 61–73. Washington DC: AGU.

Mareschal JC, Jaupart C, Cheng LZ, *et al.* (1999) Heat flow in the Trans-Hudson Orogen of the Canadian Shield: Implications for Proterozoic continental growth. *Journal of Geophysical Research* 104: 29007–29024.

Mareschal JC, Jaupart C, Gariépy C, *et al.* (2000) Heat flow and deep thermal structure near the southeastern edge of the Canadian Shield. *Canadian Journal of Earth Sciences* 37: 399–414.

Mareschal JC, Nyblade A, Perry HKC, Jaupart C, and Bienfait G (2004) Heat flow and deep lithospheric thermal structure at Lac de Gras, Slave Province, Canada. *Geophysical Research Letters* 31: L12611 (doi:10.1029/2004GL020,133).

Mareschal JC, Jaupart C, Rolandone F, *et al.* (2005) Heat flow, thermal regime, and rheology of the lithosphere in the Trans-Hudson Orogen. *Canadian Journal of Earth Sciences* 42: 517–532.

Marty JC and Cazenave A (1989) Regional variations in subsidence rate of oceanic plates: A global analysis. *Earth and Planetary Science Letters* 94: 301–315.

Maus S, Rother M, Hemant K, *et al.* (2006) Earth's lithospheric magnetic field determined to spherical harmonic degree 90 from CHAMP satellite measurements. *Geophysical Journal International* 164: 319–330.

Mayhew MA (1982) Application of satellite magnetic anomaly to Curie isotherm mapping. *Journal of Geophysical Research* 87: 4846–4854.

McDonald GJF (1959) Calculations on the thermal history of the earth. *Journal of Geophysical Research* 64: 1967–2000.

McKenzie D (1967) Some remarks on heat flow and gravity anomalies. *Journal of Geophysical Research* 72: 6261–6273.

McKenzie D (1978) Some remarks on the development of sedimentary basins. *Earth and Planetary Science Letters* 40: 25–32.

McKenzie D and Bickle MJ (1988) The volume and composition of melt generated by extension of the lithosphere. *Journal of Petrology* 29: 625–679.

McKenzie D, Jackson J, and Priestley K (2005) Thermal structure of oceanic and continental lithosphere. *Earth and Planetary Science Letters* 233: 337–349.

Michaut C and Jaupart C (2004) Nonequilibrium temperatures and cooling rates in thick continental lithosphere. *Geophysical Research Letters* 31: L24602 (doi:10.1029/2004GL021092).

Moore WB, Schubert G, and Tackley PJ (1999) The role of rheology in lithospheric thinning by mantle plumes. *Geophysical Research Letters* 26: 1073–1076.

Morgan P (1983) Constraints on rift thermal processes from heat flow and uplift. *Tectonophysics* 94: 277–298.

Nicolaysen LO, Hart RJ, and Gale NH (1981) The Vredefort radioelement profile extended to supracrustal strata at Carletonville, with implications for continental heat flow. *Journal of Geophysical Research* 86: 10653–10662.

Nielsen SB (1987) Steady state heat flow in a random medium and the linear heat flow–heat production relationship. *Geophysical Research Letters* 14: 318–322.

Nunn JA and Sleep NH (1984) Thermal contraction and flexure of intracratonic basins: A three dimensional study of the Michigan Basin. *Geophysical Journal of the Royal Astronominal Society* 79: 587–635.

Nyblade AA (1997) Heat flow across the East African Plateau. *Geophysical Research Letters* 24: 2083–2086.

Nyblade AA and Pollack HN (1993) A global analysis of heat flow from Precambrian terrains – Implications for the thermal structure of Archean and Proterozoic lithosphere. *Journal of Geophysical Research* 98: 12207–12218.

Oxburgh ER and Parmentier EM (1977) Compositional and density stratification in oceanic lithosphere; causes and consequences. *Journal of the Geological Society* 133: 343–355.

Parker RL and Oldenburg DW (1973) Geophysics–thermal model of ocean ridges. *Nature Physical Sciences* 242: 137–141.

Parsons B and McKenzie D (1978) Mantle convection and thermal structure of plates. *Journal of Geophysical Research* 83: 4485–4496.

Parsons B and Sclater JG (1977) An analysis of the variation of ocean floor bathymetry and heat flow with age. *Journal of Geophysical Research* 82: 803–827.

Perry HKC, Jaupart C, Mareschal JC, Rolandone F, and Bienfait G (2004) Heat flow in the Nipigon arm of the Keweenawan Rift, northwestern Ontario, Canada. *Geophysical Research Letters* 31: L15607 (doi:10.1029/2004GL020,159).

Perry HKC, Jaupart C, Mareschal JC, and Bienfait G (2006) Crustal heat production in the Superior Province, Canadian Shield, and in North America inferred from heat flow data. *Journal of Geophysical Research* 111: B04401 (doi:10.1029/2005JB003,893).

Pinet C, Jaupart C, Mareschal JC, Gariepy C, Bienfait G, and Lapointe R (1991) Heat flow and structure of the lithosphere in the eastern Canadian shield. *Journal of Geophysical Research* 96: 19,941–19,963.

Pollack HN (1986) Cratonization and thermal evolution of the mantle. *Earth and Planetary Science Letters* 80: 175–182.

Pollack HN and Chapman DS (1977a) On the regional variations of heat flow, geotherms, and lithospheric thickness. *Tectonophys* 38: 279–296.

Pollack HN and Chapman DS (1977b) Mantle heat flow. *Earth and Planetary Science Letters* 34: 174–184.

Pollack HN, Hurter SJ, and Johnston JR (1993) Heat flow from the earth's interior: Analysis of the global data set. *Reviews of Geophysics* 31: 267–280.

Poort J and Klerkx J (2004) Absence of a regional surface thermal high in the Baikal rift; new insights from detailed contouring of heat flow anomalies. *Tectonophysics* 383: 217–241.

Popov YA, Pribnow DFC, Sass JH, Williams CF, and Burkhardt H (1999) Characterization of rock thermal conductivity by high resolution optical scanning. *Geothermics* 28: 253–276.

Poupinet G, Arndt N, and Vacher P (2003) Seismic tomography beneath stable tectonic regions and the origin and composition of the continental lithospheric mantle. *Earth and Planetary Science Letters* 212: 89–101.

Purucker M, Langlais B, Olsen N, Hulot G, and Mandea M (2002) The southern edge of cratonic North America: Evidence from new satellite magnetometer observations. *Geophysical Research Letters* 29(9), doi:10.1029/2001GL013645.

Ramondec P, Germanovich L, Damm KV, and Lowell R (2006) The first measurements of hydrothermal heat output at 9°50'N, East Pacific Rise. *Earth and Planetary Science Letters* 245: 487–497.

Revelle R and Maxwell AE (1952) Heat flow through the floor of the eastern north Pacific ocean. *Nature* 170: 199–200.

Roberts GO (1979) Fast viscous Bénard convection. *Geophysical and Astrophysical Fluid Dynamics* 12: 235–272.

Rolandone F, Jaupart C, Mareschal JC, *et al.* (2002) Surface heat flow, crustal temperatures and mantle heat flow in the Proterozoic Trans-Hudson Orogen, Canadian Shield. *Journal of Geophysical Research* 107: 2314 (doi:10.1029/2001JB000,698).

Rolandone F, Mareschal JC, and Jaupart C (2003) Temperatures at the base of the Laurentide ice sheet inferred from heat flow data. *Geophysical Research Letters* 30(18): 1994 (doi:10.1029/2003GL018046).

Rondenay S, Bostock MG, Hearn TM, White DJ, and Ellis RM (2000) Lithospheric assembly and modification of the SE Canadian Shield: Abitibi-Grenville teleseismic experiment. *Journal of Geophysical Research* 105: 13735–13754.

Roy S and Rao RUM (2000) Heat flow in the Indian shield. *Journal of Geophysical Research* 105: 25587–25604.

Rudnick RL and Fountain DM (1995) Nature and composition of the continental crust: A lower crustal perspective. *Review of Geophysics* 33: 267–309.

Rudnick RL and Nyblade AA (1999) The thickness of Archean lithosphere: Constraints from xenolith thermobarometry and surface heat flow. In: Fei Y, Bertka CM, and Mysen BO (eds.) *Mantle Petrology; Field Observations and High Pressure Experimentation: A Tribute to Francis R. (Joe) Boyd*, pp. 3–11. Houston, TX: Geochemical Society.

Russell JK, Dipple GM, and Kopylova MG (2001) Heat production and heat flow in the mantle lithosphere, Slave craton, Canada. *Physics of the Earth and Planetary Interiors* 123: 27–44.

Sandiford M and McLaren S (2002) Tectonic feedback and the ordering of heat producing elements within the continental lithosphere. *Earth and Planetary Science Letters* 204: 133–150.

Sandwell D and Schubert G (1980) Geoid height versus age for symmetric spreading ridges. *Journal of Geophysical Research* 85: 7235–7241.

Sass JH, Lachenbruch AH, and Jessop AM (1971) Uniform heat flow in a deep hole in the Canadian shield and its paleoclimatic implications. *Journal of Geophysical Research* 76: 8586–8596.

Sass JH, Lachenbruch AH, and Galanis SP, Jr. (1994) Thermal regime of the southern Basin and Range: 1. Heat flow data from Arizona and the Mojave desert of California and Nevada. *Journal of Geophysical Research* 99: 22093–22120.

Schärmeli G (1979) Identification of radioactive thermal conductivity in olivine up to 25 kbar and 1500K. In: Timmerhaul KD and Barber MS (eds.) *Proceedings of the 6th AIRAPT Conference*, pp. 60–74. New York: Plenum.

Schutt D and Lesher C (2006) The effects of melt depletion on the density and seismic velocity of garnet and spinel

lherzolite. *Journal of Geophysical Research* 111: B05401 (doi:10.1029/2003JB002,950).
Sclater JG, Jaupart C, and Galson D (1980) The heat flow through oceanic and continental crust and the heat loss from the earth. *Reviews of Geophysics* 18: 269–311.
Seno T and Yamanaka Y (1996) Double seismic zones, compressional deep trench outer rise events, and superplumes. In: Bebout GE, Scholl DW, Kirby SH, and Platt JP (eds.) *Subduction Top to Bottom Monograph 36*, pp. 347–355. Washington, DC: AGU.
Shapiro NM and Ritzwoller MH (2004) Thermodynamic constraints on seismic inversions. *Geophysical Journal International* 157: 1175–1188.
Silver P (1996) Seismic anisotropy beneath the continents: Probing the depths of geology. *Annual Review of Earth and Planetary Sciences* 24: 385–432.
Solomatov V and Moresi L-N (2000) Scaling of time-dependent stagnant lid convection: Application to small-scale convection on the earth and other terrestrial planets. *Journal of Geophysical Research* 105: 21795–21818.
Stein CA (1995) Heat Flow of the Earth. In: Ahrens TJ (ed.) *Global Earth Physics: A Handbook of Physical Constants*, pp. 144–158.
Stein CA and Stein S (1992) A model for the global variation in oceanic depth and heat flow with lithospheric age. *Nature* 359: 123–129.
Strutt RJ (1906) On the distribution of radium in the Earth's crust and on internal heat. *Proceeding of the Royal Society of London Series A* 77: 472–485.
Thomson W (1864) On the secular cooling of the Earth. *Transaction of the Royal Society Edinburgh* 23: 295–311.
Turcotte DL and McAdoo DC (1979) Geoid anomalies and the thickness of the lithosphere. *Journal of Geophysical Research* 84: 2381–2387.
Urey HC (1964) A review of atomic abundances in chondrites and the origin of meteorites. *Reviews of Geophysics* 2: 1–34.
van der Velden AJ, Cook F, Drummond BJ, and Goleby BR (2005) Reflections on the Neoarchean: A global prespective. In: Benn K, Mareschal JC, and Condie K (eds.) *Archean geodynamics and environments*, Geophysical Monograph Series, vol. 164, pp. 255–265. Washington: AGU.
Vasseur G and Singh RN (1986) Effects of random horizontal variations in radiogenic heat source distribution on its relationship with heat flow. *Journal of Geophysical Research* 91: 10397–10404.
Vitorello I, Hamza VM, and Pollack HN (1980) Terrestrial heat flow in the Brazilian highlands. *Journal of Geophysical Research* 85: 3778–3788.
Von Herzen RP, Cordery MJ, Detrick RS, and Fang C (1989) Heat flow and the thermal origin of hot spot swells: The Hawaiian Swell revisited. *Journal of Geophysical Research* 94: 13783–13799.
Watts AB (2001) *Isostasy and Flexure of the Lithosphere*. Cambridge: Cambridge University Press.
Wiens DA and Stein S (1984) Intraplate seismicity and stresses in young oceanic lithosphere. *Journal of Geophysical Research* 89: 11442–11464.